Transportation Research Part E 125 (2019) 116–139

Contents lists available at ScienceDirect

Transportation Research Part E

journal homepage: www.elsevier.com/locate/tre

Green hub location problem

Okan Dukkanci, Meltem Peker, Bahar Y. Kara*

Department of Industrial Engineering, Bilkent University, 06800 Ankara, Turkey

ARTICLE INFO

Keywords:
Hub location
Green transportation
Second order cone programming
Perspective cuts

ABSTRACT

This paper introduces the green hub location problem that finds the best locations for hubs, assignments of demand nodes to these hubs and speed of trucks/flights so as to route the demand between any origin-destination pairs. The aim of the service provider is to minimize the total amount of emissions that depends on vehicle speed and payload while routing the deliveries within a predetermined service time limit. In this study, we first propose a nonlinear model for this problem, which is then reformulated as a second order cone programming formulation. We strengthen the new model by using perspective reformulation approach. An extensive computational study on the CAB and TR datasets demonstrates the benefits of incorporating green transportation service activities to the classic hub location problems. We also provide insights for the carrier companies by analyzing the solutions with different discount factors, service time limits and number of hubs.

1. Introduction and literature review

Hubs are special facilities which are used to consolidate and disseminate flow in many-to-many distribution systems. These facilities are largely employed in transportation, city-logistics and telecommunication systems to route demand between each origin-destination (OD) pair. Instead of providing direct connections between each OD pair, consolidating flows at hubs enables us to discount routing cost between hub facilities and use fewer links and vehicles in the network.

The aim of the basic hub location problem is to find the best locations for hubs and assignment of demand nodes to these hubs. Assigning a demand node to its nearest hub does not necessarily provide the optimal solutions although it does in the classical location problems. Therefore, the optimal assignment of demand nodes to the hubs must also be determined in the hub location problems (Alumur et al., 2012a). O'Kelly (1986a), O'Kelly (1986b), O'Kelly (1987) introduce hub location problem and present an integer programming formulation with a quadratic objective function, which is another main difference of hub location problems from the classical location problems. Later, Campbell (1994) classifies the hub location problems into four categories with respect to their objectives: *p*-hub median, the uncapacitated hub location, *p*-hub center and hub covering problems, and presents linear formulations for each of them. The first two problems have economic objectives and minimize the total cost whereas the last two can be considered as having service level objectives. The *p*-hub center problem minimizes the maximum service level between any OD pair and the hub covering problem minimizes the number of hub locations while maintaining a predetermined service level for each pair.

Alumur and Kara (2008) and Farahani et al. (2013) show that the majority of the literature on hub location problem is devoted to the first two problems. However, due to today's competitive environment, in recent years, companies pay more attention to their service levels. Travel distances or travel times can be used to measure companies' service levels and 24-h or 48-h delivery times are also offered to consumers by cargo companies (Alumur et al., 2012b). Thus, some recent studies consider both economic and service

* Corresponding author.
E-mail address: bkara@bilkent.edu.tr (B.Y. Kara).

https://doi.org/10.1016/j.tre.2019.03.005
Received 10 December 2018; Received in revised form 31 January 2019; Accepted 5 March 2019

level objectives. Lin and Chen (2004) minimize total transportation cost and determine the fleet size to meet the predetermined service commitment of carriers. Campbell (2009) finds locations of hubs and minimizes total transportation cost under distance-dependent service level constraints for truck transportation. Yaman (2009) considers a cost minimization problem with a service time bound for a hierarchical hub network with single assignment. Ishfaq and Sox (2011) also consider a cost minimization problem for a rail-road intermodal hub network under service time requirements. Alumur et al. (2012b) study hierarchical multimodal hub location problem with time-definite deliveries over a hub network that contains airline and road segments. Dukkanci and Kara (2017) add routing and scheduling decisions to the same problem discussed in Alumur et al. (2012b).

In recent years, in addition to the service level objectives, studies have started to recognize the environmental impacts of all activities of a product (e.g. production, transportation) due to the increasing effects of global warming. Green supply chain extends the classical supply chain that considers the environmental impacts of these activities. Recently, different application areas, network configurations and optimization approaches have been considered under green/sustainable supply chain and logistics concepts such as; food (perishable item) distribution with multi-objective optimization (Rahimi et al., 2017; Rohmer et al., 2019) and on a multi-echelon network (Daryanto et al., 2019), game theoretic approaches (Saberi, 2018) with green products (Zhang et al., 2018), closed-loop supply chain applications (Kaya and Urek, 2016; Zhalechian et al., 2016) in which location and inventory decisions are considered. For a comprehensive survey on sustainable supply chain problems, we refer the reader to Barbosa-Póvoa et al. (2018). One of the crucial application areas of the supply chain problems is freight transportation. Customarily, in the freight transportation problems, the main aim is to minimize a cost function that is usually proportional to the traveled distance. However, increasing concerns about the greenhouse gas emissions and global warming reveals the need for considering environmental impacts of the transportation activities, as well. Sbihi and Eglese (2010) state that by minimizing the traveled distance, one can achieve a reduction on fuel consumption and CO_2 emissions. However, they also discuss that just minimizing the total traveled distance cannot guarantee the minimum fuel consumption because other factors such as payload and vehicle speed that affect fuel consumption should also be taken into account. Demir et al. (2014) categorize these factors as vehicle, environment, traffic, driver and operations. The authors also discuss that while including these factors increases the accuracy of the estimation in the fuel consumption amount, it also increases the complexity of the fuel consumption model.

Environmental impacts of transportation activities are first discussed in relation to vehicle routing problems (Kara et al., 2007; Bektaş and Laporte, 2011). Later, they have also recognized in location problems (Khoei et al., 2017) and location-routing problems (Govindan et al., 2014; Koç et al., 2016; Tricoire and Parragh, 2017) which optimize facility location and vehicle routing decisions simultaneously. For a comprehensive survey on green network design problems, we refer the reader to Dukkanci et al. (2019). The hub location problem that is one of the network design problems has been considered by only two studies where environmental impacts of transportation activities are included. Mohammadi et al. (2014) study a sustainable hub location problem under uncertainty. The proposed problem consists of three objectives, namely minimizing transportation cost, minimizing noise pollution and minimizing the fuel consumption on arcs and at hubs. The estimation of fuel consumption is handled by Comprehensive Modal Emission Model (CMEM) in their model. The authors set vehicle speed to a constant parameter rather than being a decision of the CMEM. To deal with the uncertainty, they apply a mixed possibilistic-stochastic programming approach and to solve the model, they develop a simulated annealing method and an imperialist algorithm. Niknamfar and Niaki (2016) focus on a bi-objective hub location problem where a collaboration exists between a holding company and multiple carriers. A dual lexicographic max-min approach is used to maximize the profits of both the company and the carriers. The authors model fuel consumption as taxes for carriers in the objective function. They estimate fuel consumption and CO_2 emissions by using CMEM where payload is not considered as a decision.

Table 1 presents features of the studies that we discuss above and provides a comparison between them and our study based on the following factors: (i) the number of objective functions (single or multi), (ii) including environmental impact, (iii) using a hub network, (iv) including time related constraints, and (v,vi,vii,viii) considering vehicle speed, payload, location and routing as decisions, respectively.

To the best of authors knowledge, this is the first study that consider a hub location problem with a service time bound in which fuel consumption and CO_2 emissions are explicitly included. As discussed before, due to competitive environment, carrier companies pay attention to their service level objectives and aim to decrease the required time of routing flows. To decrease their delivery times, companies may prefer to increase vehicle speeds. Since vehicle speed and payload affect fuel consumption significantly, we consider

Table 1
Features of existing studies.

Reference	(i) Objective	(ii) Green	(iii) Hub	(iv) Time Bound	(v) Speed	(vi) Load	(vii) Location	(viii) Routing
Kara et al. (2007)	Single	✓				✓		✓
Bektaş and Laporte (2011)	Single	✓		✓	✓	✓		✓
Khoei et al. (2017)	Single	✓		✓	✓		✓	
Govindan et al. (2014)	Multi	✓		✓			✓	✓
Koç et al. (2016)	Single	✓				✓	✓	✓
Tricoire and Parragh (2017)	Multi	✓				✓	✓	✓
Mohammadi et al. (2014)	Multi	✓	✓			✓	✓	
Niknamfar and Niaki (2016)	Multi	✓	✓	✓	✓		✓	
Our Study	Single	✓	✓	✓	✓	✓	✓	

them as decisions of the CMEM to estimate fuel consumption amount accurately. Thus, including them as decisions could provide insights to the carrier companies that consider environmental impacts of their transportation activities. In this direction, we first propose a nonlinear mathematical model that minimizes total emission amount and then we reformulate the model as a second order cone programming model. We also strengthen the new model by adding perspective cuts. An extensive computational study on different datasets discusses the benefits of incorporating green transportation service activities to the hub location problem.

The remainder of this paper is organized as follows. Section 2 presents the emission model and the nonlinear mathematical formulation of the proposed problem. Section 3 provides the second order cone programming formulation. In this section, we also provide perspective cuts to strengthen the model. Computational analysis with the CAB and TR datasets and the related discussions on the results are given in Section 4. We summarize and conclude with managerial insights in Section 5.

2. Problem definition and formulation

We define the green hub location problem (GHLP) as designing a hub network that finds locations for hubs, assignments of demand nodes to these hubs, the flow (payload) carried between nodes and the speed at which vehicles travel on spoke and hub arcs. The aim of the problem is to minimize total amount of emissions which is explicitly calculated by an emission model while guaranteeing a predetermined service time bound between each OD pair. In the remainder of this section, we first briefly explain the emission model used in this paper that calculates the amount of emissions. We then provide the mathematical formulation of the GHLP.

2.1. Calculating emissions

In this study, we calculate the amount of emissions based on the Comprehensive Modal Emission Model (CMEM), which was proposed by Barth et al. (2005), Scora and Barth (2006) and Barth and Boriboonsomsin (2008) in order to estimate fuel consumption for heavy-goods vehicles. Since there is a direct relation between emission and fuel consumption, the amount of emissions can easily be obtained when the fuel consumption is calculated (Demir et al., 2014).

The total fuel consumption $F(v, M)$ (in L) of a vehicle traversing an arc of d units (in m) as a function of speed v and total weight M, can be estimated as follows:

$$F(v, M) = d(\lambda K \Upsilon V/v + \lambda\gamma M\delta + \lambda\gamma\beta v^2).$$

The expression above is explicitly included in the objective function of the mathematical model for the GHLP in the following section. The detailed explanation of the CMEM and fuel consumption ($F(v, M)$) can be found in Appendix A.1.

2.2. Model development of GHLP

The GHLP is defined on a directed complete graph $G = (N, A)$ where N denotes the demand nodes, $A = \{(i, j): i, j \in N, i \neq j\}$ denotes the set of arcs and H represents the possible hub locations ($H \subseteq N$). The following parameters and decision variables are used in the mathematical model of GHLP (Table 2). For the sake of tractability, the parameters of the emission model are given in Appendix A.2. We note that, in order to calculate emissions during the transportation correctly, we differentiate vehicle speeds on hub arcs (v^h_{km}) and spoke arcs (v^d_{ik}). To incorporate the effects of a hub network, we assume that the vehicles used between hubs will

Table 2
Nomenclature.

Parameters	
w_{ij}	demand originated from node $i \in N$ and destined to node $j \in N$
O_i	total amount of flow originated at node $i \in N$, $O_i = \sum_{j \in N} w_{ij}$
D_i	total amount of flow destined to node $i \in N$, $D_i = \sum_{j \in N} w_{ji}$
d_{ij}	distance from node $i \in N$ to node $j \in N$
α_c	hub-to-hub discount factor for the travel cost
α_t	hub-to-hub discount factor for the travel time
p	number of hubs
v_{min}	minimum travel speed
v_{max}	maximum travel speed
T	maximum service time for each OD pair
Decision Variables	
x_{ik}	1 if node $i \in N$ is allocated to hub $k \in H$, and 0 otherwise
y_i^{km}	flow originated at node $i \in N$ and routed from hub $k \in H$ to hub $m \in H$
r_k	maximum time between hub $k \in H$ and the nodes allocated to that hub
v^d_{ik}	travel speed from node $i \in N$ to hub $k \in N$
v^h_{km}	travel speed from hub $k \in N$ to hub $m \in N$

have different specifications that can affect the amount of fuel consumed and travel time. Therefore, we use two different discount factors, α_c and α_t for discounting travel cost (emissions) and travel time, respectively similar to the studies in the hub location literature.

The mixed-integer nonlinear programming formulation for the GHLP is as follows:

(GHLP-0)

$$\text{Minimize } z_1 + z_2 + z_3 + z_4 \tag{1}$$

subject to

$$z_1 = \sum_{i\in N}\sum_{k\in H} \delta\gamma\lambda d_{ik}(2\omega + O_i + D_i)x_{ik} \tag{2}$$

$$z_2 = \sum_{k\in H}\sum_{m\in H} \alpha_c\delta\gamma\lambda d_{km}\left(\omega x_{kk}x_{mm} + \sum_{i\in N} y_i^{km}\right) \tag{3}$$

$$z_3 = \sum_{i\in N}\sum_{k\in H} 2\lambda d_{ik}\left(\beta\gamma(v_{ik}^d)^2 + K\Upsilon V\frac{1}{v_{ik}^d}\right)x_{ik} \tag{4}$$

$$z_4 = \sum_{k\in H}\sum_{m\in H} \alpha_c\lambda d_{km}\left(\beta\gamma(v_{km}^h)^2 + K\Upsilon V\frac{1}{v_{km}^h}\right)x_{kk}x_{mm} \tag{5}$$

$$\sum_{k\in H} x_{ik} = 1 \qquad \forall\, i \in N \tag{6}$$

$$x_{ik} \leqslant x_{kk} \qquad \forall\, i \in N, k \in H \tag{7}$$

$$\sum_{k\in H} x_{kk} = p \tag{8}$$

$$\sum_{m\in H} y_i^{km} - \sum_{m\in H} y_i^{mk} = O_i x_{ik} - \sum_{j\in N} w_{ij}x_{jk} \qquad \forall\, i \in N, k \in H \tag{9}$$

$$\sum_{m\in H\setminus\{k\}} y_i^{km} \leqslant O_i x_{ik} \qquad \forall\, i \in N, k \in H \tag{10}$$

$$\frac{d_{ik}}{v_{ik}^d}x_{ik} \leqslant r_k \qquad \forall\, i \in N, k \in H \tag{11}$$

$$r_k + r_m + \alpha_t\frac{d_{km}}{v_{km}^h}x_{kk}x_{mm} \leqslant T \qquad \forall\, k, m \in H \tag{12}$$

$$v_{min} \leqslant v_{ik}^d \leqslant v_{max} \qquad \forall\, i \in N, k \in H \tag{13}$$

$$v_{min} \leqslant v_{km}^h \leqslant v_{max} \qquad \forall\, k, m \in H \tag{14}$$

$$x_{ik} \in \{0, 1\} \qquad \forall\, i \in N, k \in H \tag{15}$$

$$y_i^{km} \geqslant 0 \qquad \forall\, i \in N, k, m \in H \tag{16}$$

$$v_{ik}^d \geqslant 0 \qquad \forall\, i \in N, k \in H \tag{17}$$

$$v_{km}^h \geqslant 0 \qquad \forall\, k, m \in H \tag{18}$$

Objective function (1) minimizes the total amount of emissions calculated by the emission model described in Section 2.1 consisting of four terms; weight induced emissions on spoke (z_1) and hub arcs (z_2) and speed induced emissions on spoke (z_3) and hub arcs (z_4) represented by equations (2)–(5), respectively. Constraints (6) guarantee that each node is assigned to a single hub and Constraints (7) ensure that a hub is opened at a node if a node is assigned to that hub. Constraint (8) satisfies that exactly p hubs are opened. Constraints (9) guarantee flow balance at each node and Constraints (10) link the flow and assignment decision variables. Constraints (11) calculate the maximum time between a hub and the nodes that are allocated to that hub. Constraints (12) guarantee that the service time for each OD pair cannot exceed a predetermined service level, T. For service time limitations, we utilize *radius of hubs* concept (Hamacher and Meyer, 2006; Ernst et al., 2018) in Constraints (11) and (12). Constraints (13) and (14) limit travel speed on the arcs between demand node and hub, and between hubs, respectively. Constraints (15)–(18) are the domain constraints.

We remark here that, in this study, we only concentrate on total amount of emissions to show and discuss benefits of incorporating green transportation service to the hub location problem. If one aims to minimize the total cost that includes fixed, transportation and emission costs, our model can be easily adapted by only adding the costs of them to the objective function.

The proposed GHLP-0 is a mixed-integer nonlinear programming model since both objective function components (3)–(5) and

Constraints (11)–(12) have non-linear terms. To solve the problem, we first reformulate it as a second order cone programming (SOCP) model.

3. Reformulation of GHLP as a SOCP

The standard form of the Second Order Cone Programming (SOCP) is represented by Lobo et al. (1998) as follows:

$$\text{Minimize } f^T x \tag{19}$$

subject to

$$\|A_i x + b_i\|_2 \leqslant c_i^T x + d_i, \quad i = 1, \ldots, m$$
$$Fx = g$$

where $f \in \mathbb{R}^n$, $A_i \in \mathbb{R}^{n_i \times n}$, $b_i \in \mathbb{R}^{n_i}$, $c_i \in \mathbb{R}^n$, $d_i \in \mathbb{R}$, $F \in \mathbb{R}^{p \times n}$, $g \in \mathbb{R}^p$ and $\|.\|_2$ is Euclidean norm. Below, we reformulate GHLP-0 as a SOCP model. We first linearize the multiplication of two binary decision variables x_{kk} and x_{mm} by defining a new auxiliary decision variable, a_{km}. We replace $x_{kk}x_{mm}$ in the objective function components (3) and (5) and in Constraints (12) with a_{km} and add the following constraints to the GHLP-0:

$$a_{km} \leqslant x_{kk} \ \forall\, k, m \in H \tag{20}$$

$$a_{km} \leqslant x_{mm} \ \forall\, k, m \in H \tag{21}$$

$$a_{km} \geqslant x_{kk} + x_{mm} - 1 \ \forall\, k, m \in H \tag{22}$$

$$a_{km} \in \{0, 1\} \ \forall\, k, m \in H \tag{23}$$

Constraints (20) and (21) guarantee that if a hub is not located at node k or m (or both), then a_{km} is equal to 0 and if hubs are located at nodes k and m, then Constraints (22) ensure that a_{km} is equal to 1.

After linearization of $x_{kk}x_{mm}$, we introduce four new auxiliary decision variables for the remaining nonlinear terms in GHLP-0.

$$u_{ik}^d = (v_{ik}^d)^2 \ \forall\, i \in N, k \in H \tag{24}$$

$$u_{km}^h = (v_{km}^h)^2 \ \forall\, k, m \in H \tag{25}$$

$$s_{ik} = \frac{x_{ik}}{v_{ik}^d} \ \forall\, i \in N, k \in H \tag{26}$$

$$t_{km} = \frac{a_{km}}{v_{km}^h} \ \forall\, k, m \in H \tag{27}$$

We now reformulate GHLP-0 as a mixed integer SOCP by utilizing the auxiliary decision variables.

(SOCP-GHLP)

$$\text{Minimize } z_1' + z_2' + z_3' + z_4' \tag{28}$$

subject to

(6)–(10), (15)–(18), (20)–(23)

$$z_1' = z_1 = \sum_{i \in N} \sum_{k \in H} \delta\gamma\lambda d_{ik}(2\omega + O_i + D_i)x_{ik} \tag{2′}$$

$$z_2' = \sum_{k \in H} \sum_{m \in H} \alpha_c \delta\gamma\lambda d_{km}(\omega a_{km} + \sum_{i \in N} y_i^{km}) \tag{3′}$$

$$z_3' = \sum_{i \in N} \sum_{k \in H} 2\lambda d_{ik}(\beta\gamma u_{ik}^d + K\Upsilon V s_{ik}) \tag{4′}$$

$$z_4' = \sum_{k \in H} \sum_{m \in H} \alpha_c \lambda d_{km}(\beta\gamma u_{km}^h + K\Upsilon V t_{km}) \tag{5′}$$

$$(v_{ik}^d)^2 \leqslant u_{ik}^d \qquad \forall\, i \in N, k \in H \tag{29}$$

$$(v_{km}^h)^2 \leqslant u_{km}^h \qquad \forall\, k, m \in H \tag{30}$$

$$x_{ik} \leqslant s_{ik} v_{ik}^d \qquad \forall\, i \in N, k \in H: i \neq k \tag{31}$$

$$a_{km} \leqslant t_{km} v_{km}^h \qquad \forall\, k, m \in H \tag{32}$$

$$d_{ik} s_{ik} \leqslant r_k \qquad \forall\, i \in N, k \in H \tag{11′}$$

$$r_k + r_m + \alpha_t d_{km} t_{km} \leqslant T \qquad \forall\, k, m \in H \tag{12'}$$

$$v_{min} x_{ik} \leqslant v_{ik}^d \leqslant v_{max} x_{ik} \qquad \forall\, i \in N, k \in H \tag{13'}$$

$$v_{min} a_{km} \leqslant v_{km}^h \leqslant v_{max} a_{km} \qquad \forall\, k, m \in H \tag{14'}$$

Proposition 1. *There exists an optimal solution of SOCP-GHLP with the same optimal objective function value of GHLP-0.*

Proof. We first show that for every feasible solution of GHLP-0, there exists a solution in the feasible space of SOCP-GHLP with the same objective function value. We take a solution of GHLP-0 and assign the same values of decision variables to their corresponding decision variables (x, y, r, v^h and v^d) in SOCP-GHLP. By definition, $z_1 = z_1'$ and for z_2, we can safely utilize Constraints (20)–(23) without losing from optimality and z_2' will be equal to z_2. For z_3 and z_4, we differentiate based on the possible cases:

Case (i): $x_{ik} = 1$ and $v_{ik}^d > 0$.
For this case, from Equations (24) and (26), we directly find values of $u_{ik}^d = (v_{ik}^d)^2$ and $s_{ik} = x_{ik}/v_{ik}^d$, and guarantee the same value with z_3 as $(v_{ik}^d)^2 x_{ik}$ will be equal to u_{ik}^d.

Case (ii): : $x_{ik} = 0$ and $v_{ik}^d > 0$.
For this case, z_3 will be equal to 0 since $x_{ik} = 0$. There is a feasible solution in SOCP-GHLP with z_3' equal to zero, as well. For that, we can simply set the values of v_{ik}^d to zero to satisfy the Constraints (13′). We then safely set u_{ik}^d and s_{ik} to zero without violating Constraints (29) and (31), and guarantee that z_3' is also equal to zero.

Case (iii): $x_{kk} x_{mm} = 1$ and $v_{km}^h > 0$.
We first remark here that if $x_{kk} x_{mm} = 1$ then $a_{km} = 1$ by Constraints (20)–(23). Similar to Case (i), from Equations (25) and (27), we find values of $u_{km}^h = (v_{km}^h)^2$ and $t_{km} = a_{km}/v_{km}^h$ in guaranteeing the same value of z_4 for this case since $(v_{km}^h)^2 x_{kk} x_{mm}$ will be equal to u_{km}^h.

Case (iv): $x_{kk} x_{mm} = 0$ and $v_{km}^h > 0$.
In this case, z_4 will also be equal to 0 since $x_{kk} x_{mm} = 0$. There is a feasible solution in SOCP-GHLP with z_4' equal to zero. For that, we can simply set the values of v_{km}^h to zero in SOCP-GHLP in order to satisfy the Constraints (14′). We then set u_{km}^h and t_{km} to zero without violating Constraints (30) and (32), and guarantee that z_4' equals to zero, as well. By combining the four cases, we end up with a feasible solution for SOCP-GHLP with the same objective function value of GHLP-0.

We now prove that the optimal solution SOCP-GHLP is also feasible for GHLP-0. We first note that, in the optimal solution of SOCP-GHLP, Constraints (29)–(32) should be binding. (If they are not binding, decreasing the values of u_{ik}^d, u_{km}^h, s_{ik} and t_{km} reduces the optimal solution value without affecting the feasibility of the other constraints.) Then, Constraints (29)–(32) turn out to be equal to Equations (24)–(27). Thus, from the optimal solution of SOCP-GHLP, we can generate a feasible solution of GHLP-0 by removing the variables u^d, u^h, s and t. □

We next show that, Constraints (29)–(32) can be rewritten in the form of Constraint (19). Constraints (29) and (30) are quadratic inequalities and since $u_{ik}^d \geqslant 0$, $u_{km}^h \geqslant 0$, $v_{ik}^d \geqslant 0$ and $v_{km}^h \geqslant 0$, they can be rewritten as second order cone constraints in the following form:

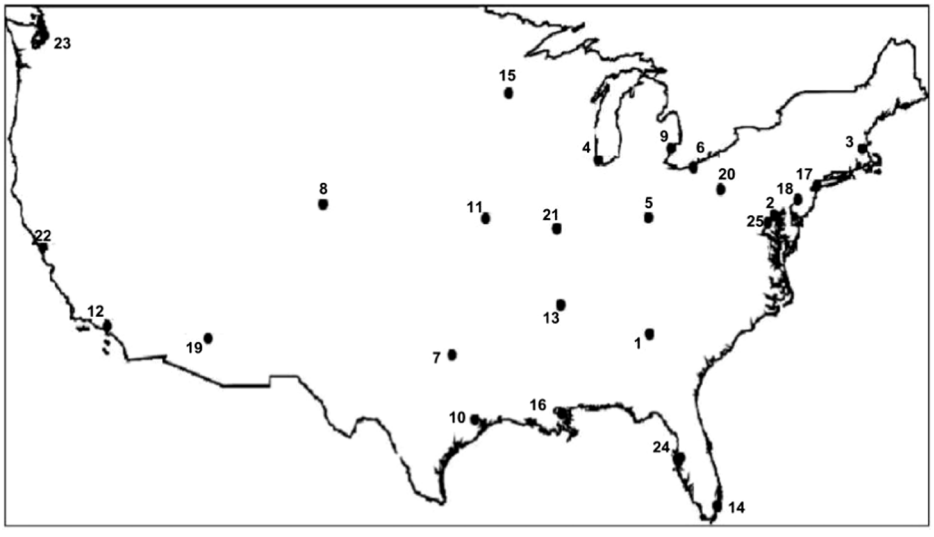

Fig. 1. Map of the US with 25 Cities.

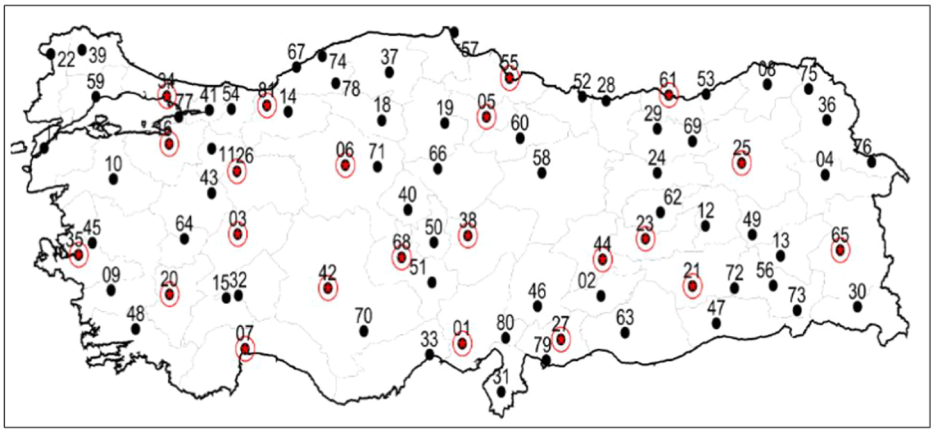

Fig. 2. Map of Turkey with cities and potential hub locations.

$$\left\| \begin{bmatrix} 2v_{ik}^{d} \\ 1 - u_{ik}^{d} \end{bmatrix} \right\| \leqslant (1 + u_{ik}^{d}) \qquad \forall\, i \in N, k \in H \tag{29'}$$

$$\left\| \begin{bmatrix} 2v_{km}^{h} \\ 1 - u_{km}^{h} \end{bmatrix} \right\| \leqslant (1 + u_{km}^{h}) \qquad \forall\, k, m \in H \tag{30'}$$

However, Constraints (31) and (32) cannot be directly rewritten as second order cone constraints. Thus, we first reformulate Constraints (31) and (32) as follows:

$$x_{ik}^{2} \leqslant s_{ik} v_{ik}^{d} \qquad \forall\, i \in N, k \in H: i \neq k \tag{33}$$

$$a_{km}^{2} \leqslant t_{km} v_{km}^{h} \qquad \forall\, k, m \in H \tag{34}$$

Constraints (33) are hyperbolic inequalities and since $x_{ik} \in \{0, 1\}$, $v_{ik}^{d} \geqslant 0$ and $s_{ik} \geqslant 0$, they can be represented as second order cone constraints in the following form:

$$\left\| \begin{bmatrix} 2x_{ik} \\ v_{ik}^{d} - s_{ik} \end{bmatrix} \right\| \leqslant (v_{ik}^{d} + s_{ik}) \qquad \forall\, i \in N, k \in H: i \neq k \tag{33'}$$

Similarly, since $a_{km} \in \{0, 1\}$, $v_{km}^{h} \geqslant 0$ and $t_{km} \geqslant 0$, Constraints (34) can also be represented as second order cone constraints in the following form:

$$\left\| \begin{bmatrix} 2a_{km} \\ v_{km}^{h} - t_{km} \end{bmatrix} \right\| \leqslant (v_{km}^{h} + t_{km}) \qquad \forall\, k, m \in H \tag{34'}$$

Table 3
Performance of the perspective cuts.

T (h)	p	GHLP-Base (s)	With PCs (s)	Imp (%)
24	5	3227.58	**2236.44**	30.71
24	6	3327.03	**2429.15**	26.99
24	7	6180.05	**3365.07**	45.55
24	8	11118.79	**4771.83**	57.08
22	5	3186.44	**2676.22**	16.01
22	6	5078.18	**2416.22**	52.42
22	7	7547.38	**2959.19**	60.79
22	8	11366.13	**4478.24**	60.60
20	5	**9574.38**	10230.59	−6.85
20	6	17794.96	**14452.02**	18.79
20	7	9289.12	**8506.75**	8.42
20	8	15747.47	**8772.71**	44.29
Average		8619.79	5607.87	34.57

Table 4
Results on the CAB dataset with different T and p values.

T (h)	p	Emission z_1' (L)	z_2' (L)	z_3' (L)	z_4' (L)	Total (L)	Av. Speed Spoke (km/h)	Hub (km/h)	Location
60	1	24.01	0.00	6.65	0.00	30.66	59.26	–	11
60	2	15.12	2.36	4.37	0.32	22.17	58.42	85.58	5,8
60	3	11.28	4.45	3.57	0.82	20.12	59.57	66.80	8,21,25
60	4	9.08	5.67	3.03	1.41	19.18	58.55	60.82	1,4,8,18
60	5	8.86	5.66	2.72	1.93	19.17	57.96	58.04	1,2,4,8,13
60	6	7.88	6.38	2.50	2.75	19.51	57.92	56.54	1,4,6,8,13,18
60	7	7.99	6.48	2.40	3.38	20.25	58.20	57.45	1,2,4,6,8,13,21
60	8	7.43	7.23	2.29	4.25	21.20	58.24	56.16	1,4,5,6,8,13,18,21
54	1	24.01	0.00	6.88	0.00	30.88	62.11	–	11
54	2	15.12	2.36	4.52	0.34	22.33	61.50	90.00	5,8
54	3	11.86	4.35	3.42	0.75	20.38	59.60	70.70	8,13,20
54	4	9.08	5.67	3.10	1.47	19.33	60.77	63.98	1,4,8,18
54	5	8.86	5.66	2.79	1.99	19.29	60.04	60.06	1,2,4,8,13
54	6	7.88	6.38	2.56	2.80	19.62	60.19	58.53	1,4,6,8,13,18
54	7	7.99	6.48	2.46	3.43	20.37	60.56	57.60	1,2,4,6,8,13,21
54	8	7.87	6.88	2.39	4.17	21.31	60.63	56.90	1,2,4,5,6,8,13,21
48	1					Infeasible			
48	2					Infeasible			
48	3	11.86	4.35	3.56	0.82	20.59	62.49	77.35	8,13,20
48	4	9.28	5.67	3.18	1.46	19.59	62.69	67.61	4,8,13,18
48	5	8.86	5.66	2.92	2.08	19.51	63.33	63.38	1,2,4,8,13
48	6	7.88	6.38	2.70	2.89	19.84	63.79	61.06	1,4,6,8,13,18
48	7	7.55	6.82	2.55	3.63	20.55	64.09	59.27	1,4,6,8,13,18,21
48	8	7.43	7.23	2.47	4.38	21.52	64.25	58.08	1,4,5,6,8,13,18,21

The reformulated version of the problem is as follows:
(GHLP-Base)
Minimize (28)
subject to

(2′)–(5′), (6)–(10), (11′)–(14′), (15)–(18), (20)–(23), (29)–(30), (33)–(34).

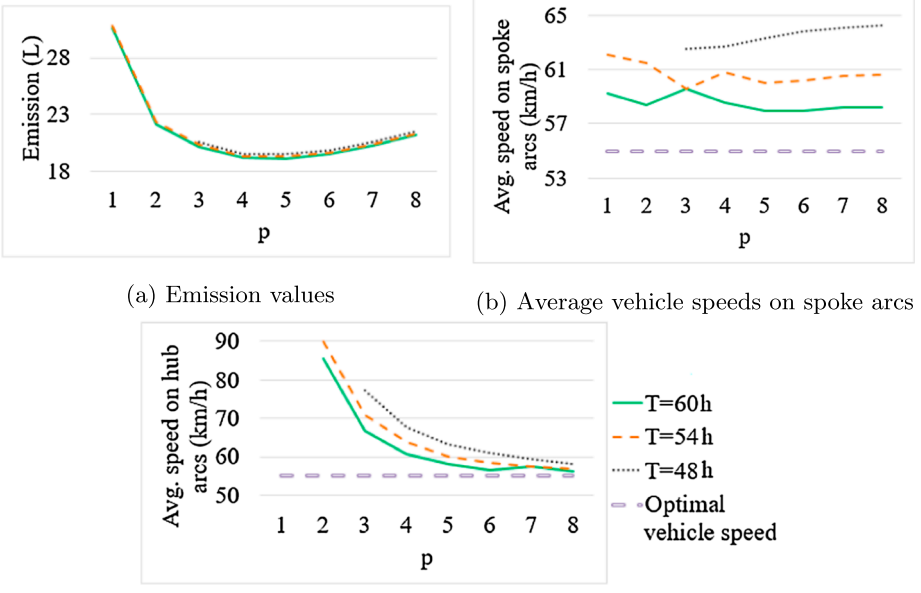

(a) Emission values

(b) Average vehicle speeds on spoke arcs

(c) Average vehicle speeds on hub arcs

Fig. 3. Schematic representation of results on the CAB dataset.

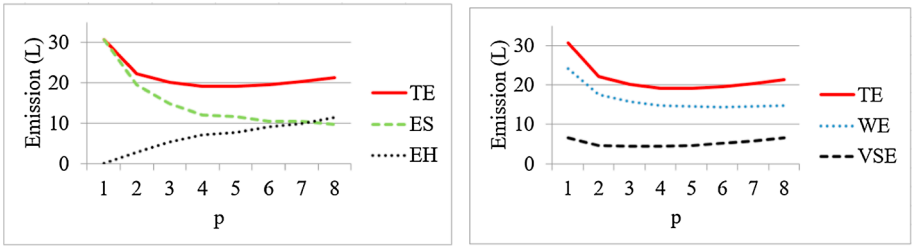

(a) Emissions on hub arcs (EH) and spoke arcs (ES)

(b) Weight induced emission (WE) and speed induced emission (VSE)

Fig. 4. Schematic representation of emission analysis on the CAB dataset with $T = 60$ hours.

3.1. Perspective cuts

To strengthen the formulation, we utilize the perspective cuts proposed by Günlük and Linderoth (2012) for the quadratic inequalities. Instead of Constraints (29) and (30), we add the following perspective cuts to GHLP-Base:

$$(v^d_{ik})^2 \leqslant u^d_{ik} x_{ik} \qquad \forall\, i \in N, k \in H \tag{35}$$

$$(v^h_{km})^2 \leqslant u^h_{km} a_{km} \qquad \forall\, k, m \in H \tag{36}$$

Constraints (35) and (36) are also hyperbolic inequalities and they can be represented as second order cone constraints in the following forms:

$$\left\| \begin{bmatrix} 2v^d_{ik} \\ u^d_{ik} - x_{ik} \end{bmatrix} \right\| \leqslant (u^d_{ik} + x_{ik}) \qquad \forall\, i \in N, k \in H \tag{35′}$$

$$\left\| \begin{bmatrix} 2v^h_{km} \\ u^h_{km} - a_{km} \end{bmatrix} \right\| \leqslant (u^h_{km} + a_{km}) \qquad \forall\, k, m \in H \tag{36′}$$

(a) T = 60 hours

(b) T = 48 hours

Fig. 5. Results on the CAB dataset with three hubs.

4. Computational study

In this section, we present an extensive computational analysis on the GHLP. We first introduce the CAB and the TR datasets that are used in the computational experiments. We then evaluate the performance of the perspective cuts on the GHLP-Base and analyze the solutions of the proposed model by varying several parameters such as maximum service time (T), the number of hubs (p), hub-to-hub discount factor for the travel cost (α_c) and for travel time (α_t). We also provide a comparison between the solutions of the GHLP and the p-hub median problem to discuss the benefits of incorporating environmental considerations into a hub location problem. All experiments are implemented in a Java platform using Cplex 12.7.1 on a Linux OS environment with Dual Intel Xeon E5-2690 v4 14 Core 2.6 GHz processors with 128 GB of RAM.

4.1. Datasets

In the computational experiments, we use the US Civil Aeronautics Board (CAB) and Turkish network (TR) datasets. The CAB dataset is based on airline passenger interactions between 25 US cities in 1970 (O'Kelly, 1987). Fig. 1 shows the locations of the 25 cities that represent the demand nodes and the potential hubs ($|N| = |H| = 25$). For more information on the CAB dataset, we refer the reader to Beasley (2012).

The TR dataset introduced by Tan and Kara (2007) consists of 81 cities in Turkey. The location of these cities are shown in Fig. 2, where each city is considered as a demand node ($|N| = 81$). There are 22 potential hub nodes ($|H| = 22$), presented with red and big circles on the map.

For both datasets, the hub-to-hub discount factors for travel cost (α_c) and travel time (α_t) are taken as 0.75 and 0.8, respectively (Alumur et al., 2009). The minimum (v_{min}) and maximum (v_{max}) speed limits are set to 10 km/h and 90 km/h, respectively.

Table 5
Results on the TR dataset with different T and p values.

		Emission					Av. Speed		
T (h)	p	z_1' (L)	z_2' (L)	z_3' (L)	z_4' (L)	Total (L)	Spoke (km/h)	Hub (km/h)	Location
24	1	69.87	0.00	9.45	0.00	79.31	59.85	–	38
24	2	47.56	10.67	6.51	0.13	64.87	58.84	90.00	6,44
24	3	42.59	12.59	5.78	0.29	61.26	58.32	66.79	1,6,23
24	4	34.26	18.12	4.97	0.61	57.95	58.04	65.29	1,6,23,26
24	5	26.86	22.13	4.54	1.06	54.59	57.74	63.35	1,3,6,23,34
24	6	23.86	23.45	4.07	1.45	52.82	56.97	59.34	1,3,5,6,23,34
24	7	22.78	23.78	3.87	1.83	52.26	56.93	58.05	1,3,5,6,23,34,68
24	8	21.05	24.92	3.35	2.66	51.98	56.65	57.28	1,3,5,6,23,25,34,68
24	9	18.29	26.81	3.55	3.30	51.95	57.52	57.56	1,3,5,6,16,23,34,35,68
24	10	17.66	27.13	3.42	3.93	52.14	57.68	57.21	1,3,5,6,16,23,34,35,68,81
24	11	16.26	28.21	3.28	4.83	52.57	57.79	56.96	1,3,6,16,23,34,35,38,42,55,81
24	12	14.61	29.62	2.77	6.33	53.33	57.31	56.51	1,3,6,16,23,25,34,35,38,42,55,81
22	1						Infeasible		
22	2	47.29	11.10	6.66	0.13	65.18	61.36	90.00	6,44
22	3	42.15	13.12	5.88	0.29	61.44	60.59	66.79	1,6,23
22	4	34.26	18.12	5.13	0.61	58.12	60.60	66.56	1,6,23,26
22	5	26.41	22.63	4.53	1.10	54.68	58.92	65.70	1,3,6,23,34
22	6	23.84	23.48	4.11	1.49	52.91	58.32	61.61	1,3,5,6,23,34
22	7	22.78	23.78	3.92	1.87	52.35	58.30	59.63	1,3,5,6,23,34,68
22	8	21.05	24.92	3.39	2.71	52.06	57.78	58.84	1,3,5,6,23,25,34,68
22	9	18.29	26.81	3.61	3.36	52.06	58.86	58.93	1,3,5,6,16,23,34,35,68
22	10	17.64	27.16	3.46	4.00	52.26	59.11	58.38	1,3,5,6,16,23,34,35,68,81
22	11	17.05	27.57	3.42	4.67	52.70	59.20	57.81	1,3,5,6,16,23,34,35,42,68,81
22	12	14.61	29.62	2.81	6.41	53.45	58.63	57.62	1,3,6,16,23,25,34,35,38,42,55,81
20	1						Infeasible		
20	2						Infeasible		
20	3						Infeasible		
20	4						Infeasible		
20	5	30.33	23.60	4.69	1.43	60.06	61.61	73.72	21,25,26,34,68
20	6	27.51	23.63	4.31	1.88	57.33	61.51	70.93	6,21,25,26,34,68
20	7	21.52	25.61	3.71	2.61	53.45	60.60	68.06	1,3,6,16,21,34,61
20	8	20.12	25.94	3.37	3.19	52.62	60.02	63.37	1,3,5,6,16,21,25,34
20	9	19.17	26.26	3.22	3.80	52.43	59.92	61.38	1,3,5,6,16,21,25,34,68
20	10	17.68	27.23	3.05	4.61	52.57	59.78	59.92	1,3,6,16,21,25,34,38,42,55
20	11	16.23	28.37	2.87	5.57	53.04	59.62	58.88	1,3,6,16,21,25,27,34,38,42,55
20	12	15.58	28.91	2.72	6.54	53.75	60.01	58.58	1,3,6,16,21,25,27,34,38,42,55,81

4.2. Performance of perspective cuts

This section presents the results of experiments conducted on the performance of the proposed perspective cuts (35) and (36). In these experiments, we consider the TR dataset with three different T values (24, 22, 20) in hours and four different p values (5, 6, 7, 8), in total 12 instances which are considered as the most difficult cases in our test instances. Table 3 depicts the results where the first two columns represent the maximum service time (T) in hours and the number of hubs (p). The next two columns titled "GHLP-Base" and "With PCs" show the solution times of the formulation without and with perspective cuts in seconds, respectively. The last column titled "Imp (%)" shows the solution time improvement of including perspective cuts in percentages. The last row indicates the average solution time of the 12 instances for both versions of the formulation.

The results in Table 3 show that including the proposed perspective cuts into the model reduces the solution times in all 12 instances except one. For some instances the improvement increases up to 57%. Since, on average, the formulation with perspective cuts reduces the solution time by 34.57%, we use these cuts and include them into the formulation in the rest of the experiments.

4.3. Computational analysis

In this section, we present a comprehensive computational analysis on the solutions of the GHLP to evaluate the impacts of several key parameters of the problem. First, we analyze the effects of the maximum service time (T) and the number of hubs (p) on the CAB dataset where T is set as 60, 54 and 48 h and p is varied between one and eight. The results can be found in Table 4 which presents the total emission amount (in L) and components of it in terms of weight induced emissions on spoke (z_1') and hub arcs (z_2') and speed induced emissions on spoke (z_3') and hub arcs (z_4'). Table 4 also demonstrates the average vehicle speeds on spoke and hub arcs (in km/h) and hub locations, respectively.

The results in Table 4 suggest that for tighter maximum service time, for the same p the total amount of emissions increases along with the average vehicle speed on both spoke and hub arcs (Fig. 3). We also observe that for a fixed T, the average vehicle speed on spoke arcs does not show a particular trend over the number of hubs (Fig. 3b) whereas the average vehicle speed on hub arcs reduces as p increases (Fig. 3c). We note that, if there is no service level requirements, the optimal vehicle speeds are equal to 55 km/h (Demir et al., 2012). Although decreasing travel time bound increases the vehicle speed on hub arcs, opening more hubs decreases the average speeds which approach to 55 km/h for all time bounds (Fig. 3c).

We also observe that the amount of emissions behaves like a convex function on the number of hubs. Initially, increasing p value reduces the emission amount, but after a certain p, it starts to increase (Fig. 3a). In our test instances, this certain p value for the CAB dataset is five for each T value as it can be observed in Table 4. We further analyze the results to understand the underlying reason behind the convexity of the total emission amount (TE $= z_1' + z_2' + z_3' + z_4'$) on the number of hubs. The results in Table 4 show that in general a higher p value reduces the amount of emissions on spoke arcs (ES $= z_1' + z_3'$), but it increases the emission amount on hub arcs (EH $= z_2' + z_4'$). This is consistent as higher p values reduces the number of spoke arcs and increases the number of hub arcs. Up to a certain p value, since the increase in the EH is less than the decrease in ES, total emission reduces. After that certain p value, opening new hubs does not change the assignment of demand nodes to hubs dramatically and leads to a smaller gain in ES. On the other hand, this behaviour substantially increases the number of hub arcs and thus leads to a higher increase in EH than the decrease

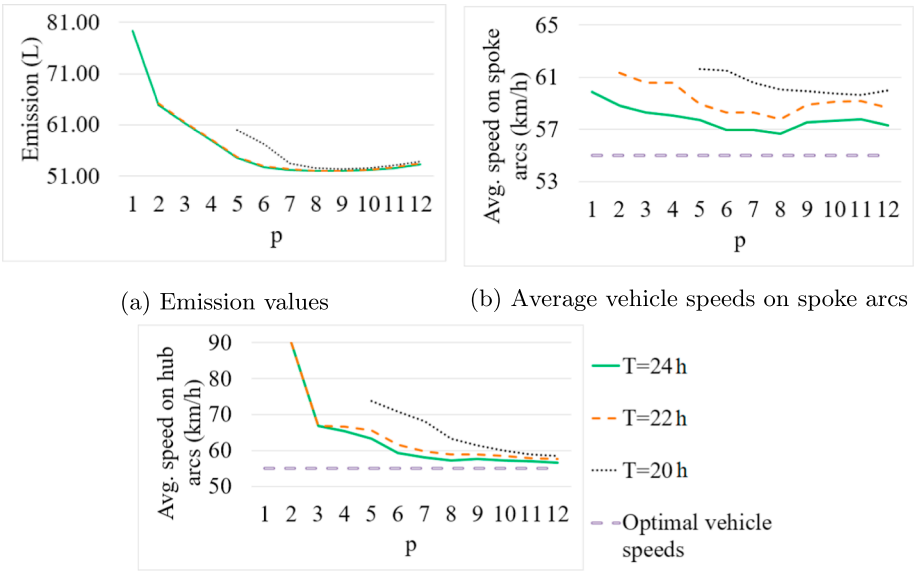

(a) Emission values

(b) Average vehicle speeds on spoke arcs

(c) Average vehicle speeds on hub arcs

Fig. 6. Schematic representation of the solutions on the TR dataset.

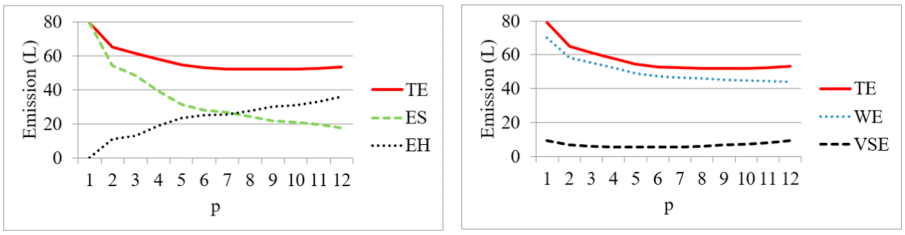

(a) Emissions on hub arcs (EH) and spoke arcs (ES)

(b) Weight induced emission (WE) and vehicle speed induced emission (VSE)

Fig. 7. Schematic representation of emission analysis on the TR dataset with $T = 24$ hours.

in ES. Therefore, the total amount of emissions acts as a convex function as it is depicted in Fig. 4a when T is set to 60 h.

We also analyze the behaviour of the weight induced emission (WE $= z_1' + z_2'$) and vehicle speed induced emission (VSE $= z_3' + z_4'$) on the number of hubs in Fig. 4b, which demonstrates that VSE and WE also behave like convex functions on the number of hubs. While the least WE amount is obtained when $p = 6$, the least VSE amount is obtained when $p = 3$ when the total emission amount is minimized. Fig. 4b also shows that the WE amount is higher than the VSE amount suggesting that z_1' and z_2' (WE) are more dominant in the objective function compared to the z_3' and z_4' (VSE).

We further analyze two instances in more detail to observe the changes on the solutions in terms of the hub locations and demand node assignments. Here, we consider instances with two different T values and the number of hubs is equal to three in both instances (Fig. 5).

When the maximum service time is set to 60 h, three hubs are opened in Denver (8), St. Louis (21) and Washington (25). Cities located in the west, center and east are assigned to Denver (8), St. Louis (21) and Washington (25), respectively (Fig. 5a). For a 48-h service time, while Denver (8) remains as a hub, other two hubs are located in Memphis (13) and Pittsburgh (20). In this case, some of the cities located in the eastern side of the US (Miami (14) and Tampa (24)) are now assigned to a centrally located hub, Memphis (13) (Fig. 5b). As it can also be seen on the maps, hubs are selected from the centrally located cities for both cases.

We also conduct experiments on the TR dataset to analyze the effect of the maximum service time and the number of hubs on the solutions. We set T to 24, 22 and 20 h and vary number of hubs (p) between one to 12 to observe the behaviour of total emission on the number of hubs. We report the results in Table 5 and the observations are very similar to the ones obtained from the experiments

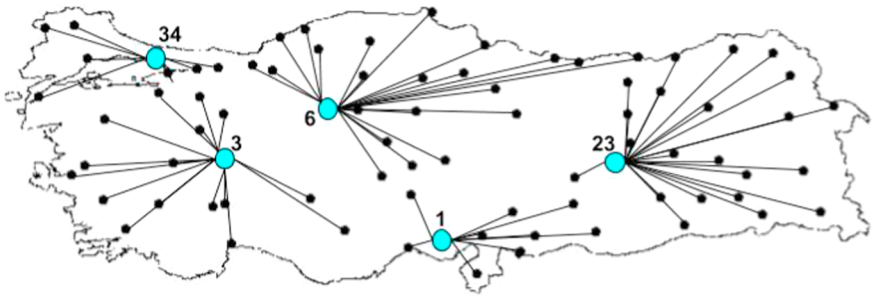

(a) T = 24 hours

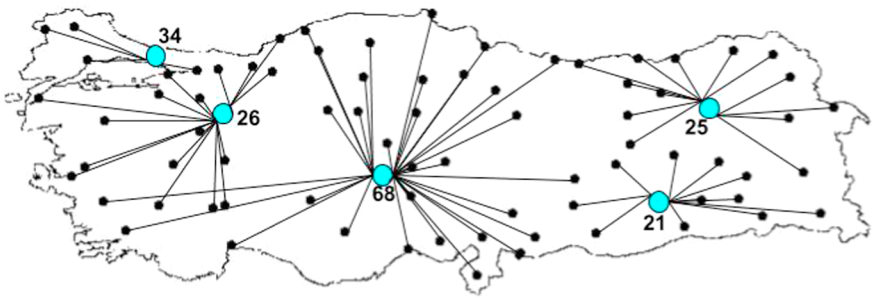

(b) T = 20 hours

Fig. 8. Results on the TR instance with five hubs.

on the CAB dataset, especially in terms of the impact of the maximum service time on the solution and convex behaviour of the total emission (Fig. 6a). We observe that the number of hubs that provides the least amount of emissions is nine for each T value (as opposed to five for the CAB dataset). Thus, for the TR data set, we need to open more hubs to obtain the minimum emission amount. Since there are more demand nodes in the TR dataset (81) than the number of nodes in the CAB dataset (25), opening a new hub in the TR dataset is more likely to change the assignments of demand nodes and reduces the emission on spoke arcs. Therefore, we observe that total emission amount decreases up to a higher p value if there are more demand nodes.

Similar to the results obtained from the experiments on the CAB dataset, the results on Table 5 suggest that the average vehicle speeds on spoke arcs do not show a particular pattern (Fig. 6b), but the average vehicle speed on hub arcs decreases as p increases (Fig. 6c). For a fixed value of p, reducing time bound increases the total amount of emissions and also the average vehicle speed on both spoke and hub arcs, as expected (Fig. 6).

Fig. 7 provides an analysis on the distribution of total emission amount when the time bound is set to 24 h. As it can be seen from Fig. 7a, increasing p value reduces the amount of emissions on spoke arcs (ES) and increases the amount of emissions on hub arcs resulting a convex function of total amount of emissions (TE) similar to the results in the CAB dataset. Fig. 7b indicates that weight induced emission (WE) amount is higher compared to the vehicle speed induced emission (VSE) for the results of the TR dataset, as well.

We also provide a further analysis on the solutions of the GHLP with different service time levels on the TR dataset. Fig. 8 presents the GHLP solutions with five hubs and service times are set to 24 and 20 h, respectively. For a 24-h service time, hubs are located in Adana (1), Afyon (3), Ankara (6), Elazig (23) and Istanbul (34) as represented in Fig. 8a. To complete all deliveries within 20 h, more dispersed locations are selected as hubs such as Diyarbakir (21), Erzurum (25), Eskisehir (26) and Aksaray (68) while Istanbul is still used as a hub due to its high O_i and D_i values (Fig. 8b).

4.3.1. Impact of α_c

In this section, we analyze the impact of hub-to-hub discount factor for the travel cost (α_c) on the solutions. We first conduct experiments on the CAB dataset with three different α_c values, namely, 0.75, 0.50 and 0.25. We report the detailed results for

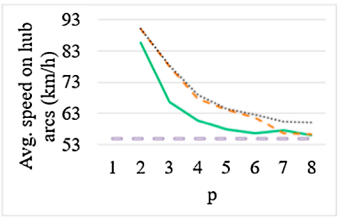

(a) Average vehicle speeds on hub arcs for T=60 h

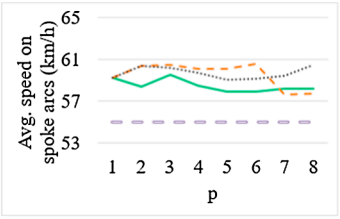

(b) Average vehicle speeds on spoke arcs for T=60 h

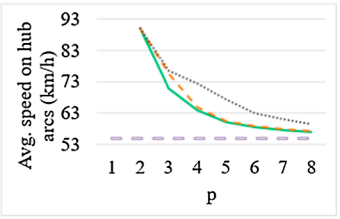

(c) Average vehicle speeds on hub arcs for T=54 h

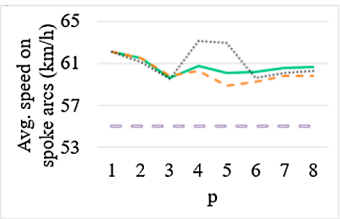

(d) Average vehicle speeds on spoke arcs for T=54 h

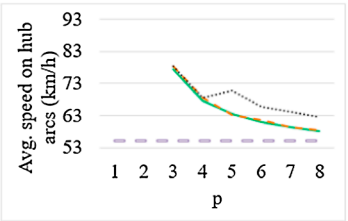

(e) Average vehicle speeds on hub arcs for T=48 h

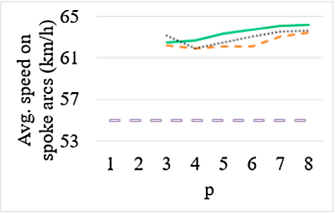

(f) Average vehicle speeds on spoke arcs for T=48 h

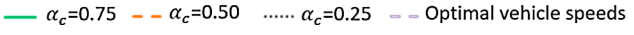

Fig. 9. Schematic representation of α_c analysis on the CAB dataset.

different service times and number of hubs in Appendix B.1. We remind the reader that the results with $\alpha_c = 0.75$ are the solutions discussed in the previous section. As α_c is a part of objective function, it directly affects the total amount of emissions thus, we do not report those values in Appendix B.1.

The results indicate that decreasing α_c generally changes the hub locations and yields more dispersed hubs. For instance, whereas none of the nodes at the west part of US (i.e. 12, 19, 22, 23) are selected as hubs in the solutions with $\alpha_c = 0.75$, Los Angeles (12) is selected as one of the hubs in most of the instances with $\alpha_c = 0.25$. Moreover, due to the changes in the hub locations, average vehicle speeds on the hub and spoke arcs are also affected. Fig. 9 visualizes the solutions in Appendix B.1 and demonstrates that the average vehicle speed on spoke arcs does not show a particular trend over α_c. However, for any T, decreasing α_c generally increases the average vehicle speed on the hub arcs by utilizing discounting cost property between hub locations. Reducing α_c from 0.75 to 0.5 and 0.25 increases the average vehicle speed on hub arcs by 2.15 km/h (3.35%) and 4.98 km/h (7.75%), respectively.

We carry out the same analysis on the TR dataset and present the detailed results in Appendix B.2. The results and deductions about the hub locations obtained here are very similar to the ones for the CAB dataset, and for the TR dataset reducing the discount factor α_c from 0.75 to 0.5 and 0.25 increases the average vehicle speed on the hub arcs by 2.46 km/h (3.67%) and 3.85 km/h (5.75%). The only difference that we observe from Fig. 10 which visualizes the solutions in Appendix B.2, decreasing α_c generally reduces the average vehicle speed on the spoke arcs.

4.3.2. Impact of α_t

In this section, we provide a detailed analysis on the impact of the hub-to-hub discount factor for the travel time (α_t), where we consider three different α_t values; 0.8, 0.6 and 0.4. We remind the reader that the results with $\alpha_t = 0.8$ are the solutions that are already discussed.

We first conduct experiments on the CAB dataset and provide the detailed results in Appendix C.1. We note that although α_t is not a part of the objective function, due to the changes in the hub locations, assignments of demand nodes and vehicle speeds, the total emission amount decreases as α_t reduces. When the discount factor is set to 0.6 and 0.4, the reduction in the emission is 0.12 L (0.58%) and 0.22 L (1.03%), respectively. The results also suggest that reducing α_t decreases the average vehicle speeds on both

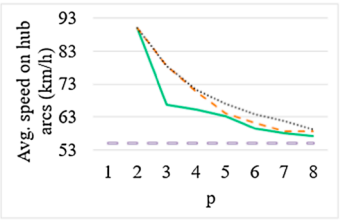

(a) Average vehicle speeds on hub arcs for T=24 h

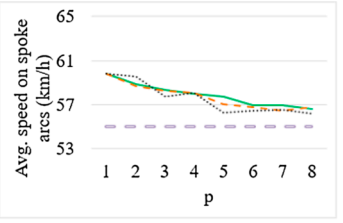

(b) Average vehicle speeds on spoke arcs for T=24 h

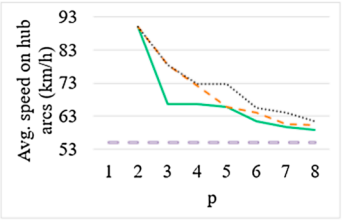

(c) Average vehicle speeds on hub arcs for T=22 h

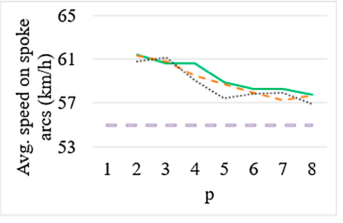

(d) Average vehicle speeds on spoke arcs for T=22 h

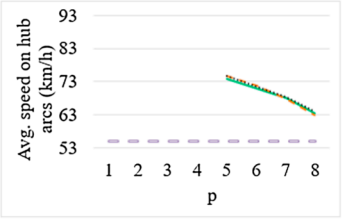

(e) Average vehicle speeds on hub arcs for T=20 h

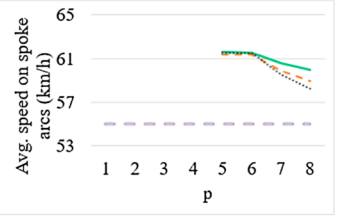

(f) Average vehicle speeds on spoke arcs for T=20 h

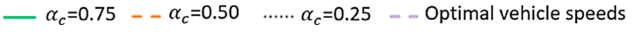

Fig. 10. Schematic representation of α_c analysis on the TR dataset.

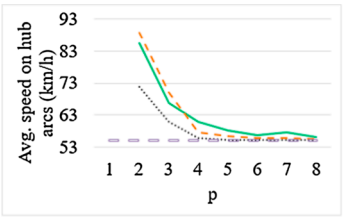

(a) Average vehicle speeds on hub arcs for T=60 h

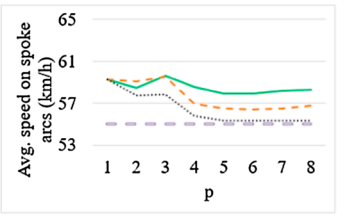

(b) Average vehicle speeds on spoke arcs for T=60 h

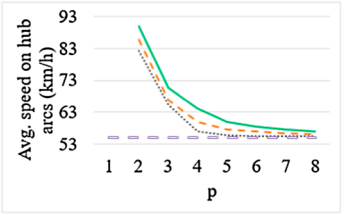

(c) Average vehicle speeds on hub arcs for T=54 h

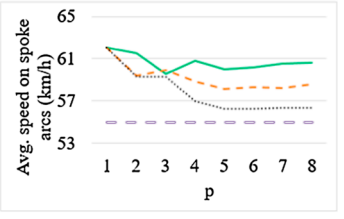

(d) Average vehicle speeds on spoke arcs for T=54 h

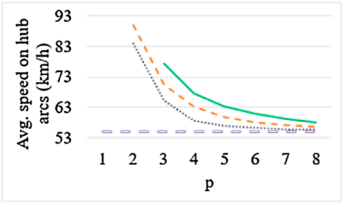

(e) Average vehicle speeds on hub arcs for T=48 h

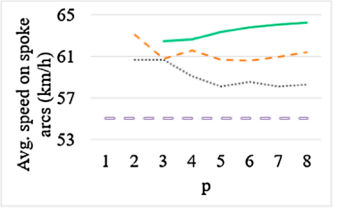

(f) Average vehicle speeds on spoke arcs for T=48 h

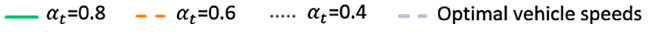

Fig. 11. Schematic representation of α_t analysis on the CAB dataset.

spoke and hub arcs (Fig. 11). By decreasing α_t, we relax the service level requirement of each OD pair and thus, vehicle speeds approach to 55 km/h (the optimal vehicle speed if there is no service level requirements). The impact of α_t on the vehicle speed on hub arcs is greater than the one on the spoke arcs. Setting α_t to 0.6 and 0.4 reduces the average vehicle speed on the spoke arcs by 1.53 km/h (2.52%) and 3.02 km/h (4.98%), respectively. These figures for the average vehicle speed on hub arcs are 2.08 km/h (3.23%) and 5.06 km/h (7.56%). In addition, reducing α_t affects the locations of hubs and in almost half of the instances, at least one of the hub locations is changed when α_t is reduced. Moreover, as α_t affects the feasibility of the problem, we obtain a feasible solution by reducing α_t for one of the infeasible solutions obtained with $\alpha_t = 0.8$.

We also carry out experiments on the TR dataset and present the results in Appendix C.2. The results show that although decreasing α_t does not affect hub locations significantly, it highly affects vehicle speeds on spoke and hub arcs. Decreasing α_t relaxes service time between each OD pair and vehicle speeds approach to 55 km/h (Fig. 12). Decreasing α_t to 0.6 and 0.4 also results with a reduction of 1.59 km/h (2.69%) and 2.56 km/h (4.33%) on the average vehicles speed on spoke arcs, respectively. The same figures for the average vehicle speed on hub arcs are 3.34 km/h (4.99%) and 6.15 km/h (9.18%). Thus, the total emission amount is also affected and reduced by 0.7 L (1.21%) and 0.77 L (1.33%) when α_t is set to 0.6 and 0.4, respectively. In addition, the results present that α_t has more impact on the feasibility of the problem with the TR dataset than the impact on the CAB dataset as we obtain three more feasible solutions with $\alpha_t = 0.6$ and $\alpha_t = 0.4$ for the infeasible solutions with $\alpha_t = 0.8$.

4.4. Comparison of GHLP and p-hub median problem

The GHLP can be considered as an extension of the classical *p*-hub median problem (*p*-HMP) where the aim is to minimize the total travel cost without any service level requirements. To evaluate considering environmental impact of emissions on the solutions, we compare the results of GHLP and a two-stage *p*-HMP. In the two-stage *p*-HMP, we first solve the *p*-HMP with a service time limit in order to decide the hub locations and demand node assignments. To ensure feasible solutions for the *p*-HMP, in this stage, we assume that vehicles travel with maximum available speed (v_{max}) on both hub and spoke arcs. After solving the *p*-HMP, we solve the GHLP-Base in which hub locations and demand node assignments are fixed to decide the vehicle speeds and to minimize the total emission amount. We compare solutions of these two problems on the CAB and TR datasets and analyze the results for different parameters.

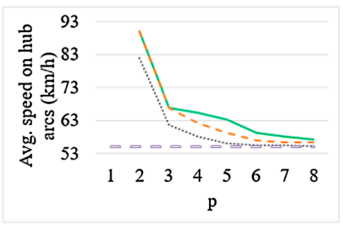

(a) Average vehicle speeds on hub arcs for T=24 h

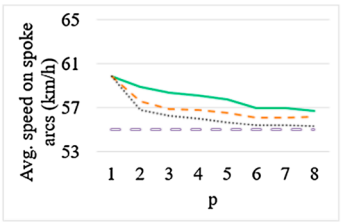

(b) Average vehicle speeds on spoke arcs for T=24 h

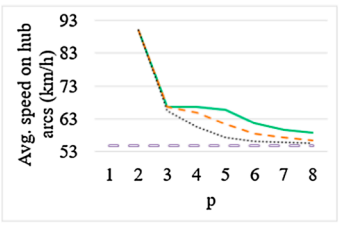

(c) Average vehicle speeds on hub arcs for T=22 h

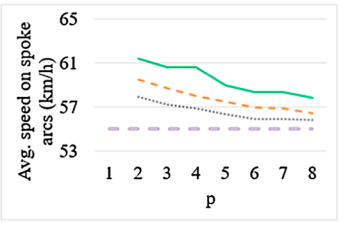

(d) Average vehicle speeds on spoke arcs for T=22 h

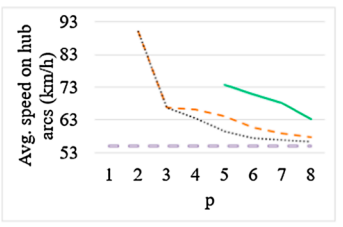

(e) Average vehicle speeds on hub arcs for T=20 h

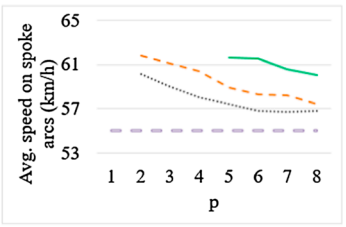

(f) Average vehicle speeds on spoke arcs for T=20 h

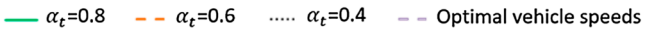

Fig. 12. Schematic representation of α_t analysis on the TR dataset.

Appendix D.1 presents the results of GHLP and two-stage *p*-HMP for the CAB dataset. The solutions indicate that in 17 out of 22 instances (two instances are infeasible), the two problems yield different results in terms of hub locations and demand node assignments. For those instances, on the average, the GHLP reduces the total amount of emissions by 5.63%. Higher p and lower T values leads to a larger reduction on the emission amount with a maximum reduction of 14.70%.

We further analyze one instance ($T = 48$ h, $p = 5$) and the solutions of two aforementioned problems are depicted in Fig. 13. In the solution of the *p*-HMP, Atlanta (1), Chicago (4), Los Angeles (12), Philadelphia (18) and Seattle (23) are opened as hubs. On the other hand, in the solution of the GHLP, Atlanta (1) and Chicago (4) remain as hubs and the other three hubs are located in Baltimore (2), Denver (8) and Memphis (13). Fig. 13 demonstrates that hubs in the solutions of the GHLP are much closer to each other compared to the hubs obtained in the solutions of the *p*-HMP. Moreover, while in the latter problem two hubs are opened in the west coast (Los Angeles (12) and San Francisco (22)), in the former one Denver (8) serves as hubs to cover demand points in the west.

As it can also be seen from Appendix D.1, the *p*-HMP generally locates the hubs based on the total incoming and outgoing flow amounts of nodes. For instance, three cities (New York (17), Los Angeles (12) and Chicago (4)) which have the highest O_i or D_i values are opened as hubs in most of the instances. On the other hand, the GHLP usually locates the hubs based on their spatial locations. The hub locations in the solutions of the GHLP are tend to be more centrally located compared to the ones in the solutions of the *p*-HMP. The main reason for this tendency is that the GHLP includes objective function components that are based on not only payload, but also vehicle speed.

We present the same analysis on the TR dataset and give the results in Appendix D.2. The results show that in seven out 19 instances (five instances are infeasible), these two problems provide different results with respect to hub locations. However, in all but except two instances ($T = 24$ h, $p = 1$ and $T = 22$ h, $p = 2$), demand node assignments are different from each other, since the total emission amounts are different for the two problems. Therefore, for the TR dataset, on the average, the GHLP reduces the total amount of emissions by 0.45%. We can conclude that although the impact of incorporating environmental consideration into the hub location problem with the TR dataset is not as high as the one on the CAB dataset, hub locations and demand node assignments change significantly in the solutions with the TR dataset. Moreover, contrary to the results obtained with the CAB dataset, lower T values provide lesser reductions on the total amount of emissions.

(a) Two stage p-HMP

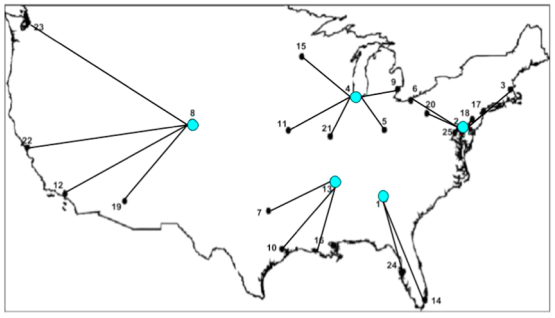

(b) GHLP

Fig. 13. Results on the CAB dataset with a 48-h service time and five hubs.

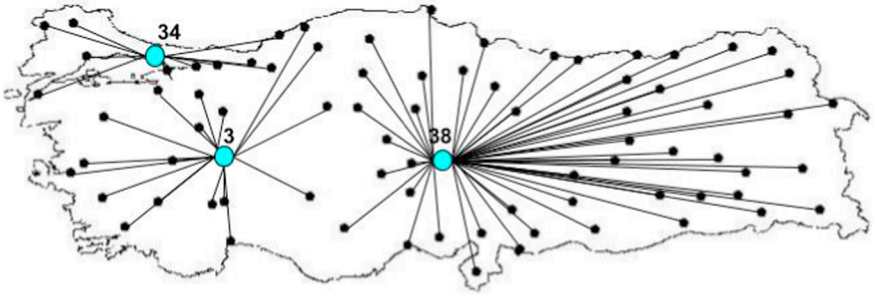

(a) Two-stage p-HMP

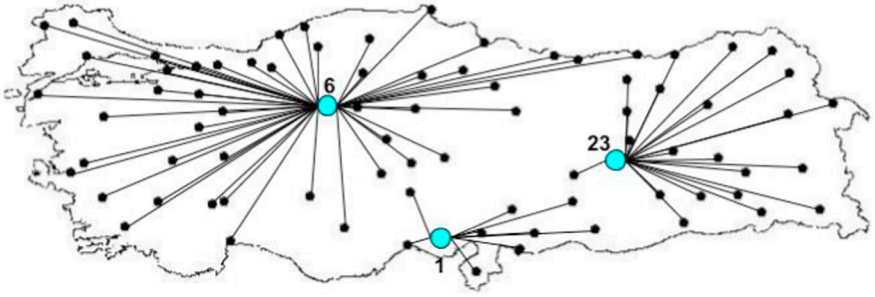

(b) GHLP

Fig. 14. Results on the TR dataset with a 24-h service time and three hubs.

We also present the solutions of these two problems for one particular instance ($T = 24$ h, $p = 3$) in Fig. 14. The p-HMP locates three hubs in Afyon (3), Istanbul (34) and Kayseri (38) and most of the demand points (51 out of 81) are assigned to Kayseri (Fig. 14a). On the other hand, in the GHLP solution, hubs are located in Adana (1), Ankara (6) and Elazig (23), and in this instance,

more than half of the demand points (48 out of 81) are assigned to Ankara (6). These two maps also show that in the solution of the p-HMP, no hub is opened in the east side of Turkey, whereas in the solution of the GHLP, no hub is opened in the west side of Turkey. As most of the population is located in the western side, O_i and D_i values are higher in that region. Therefore, while the p-HMP favors the cities located in the western side as potential hubs, the GHLP selects cities as hubs based on their spatial locations in order to optimize the vehicle speeds along with the flow variables. This pattern can also be observed in other instances in Appendix D.2. For instance, in the instance with $T = 24$ h and $p = 8$, while the p-HMP opens hubs in Bursa (16) and Izmir (35), which are located in the west, the GHLP selects hubs from eastern region, Erzurum (25) and Aksaray (68).

5. Conclusion

In this study, we proposed the Green Hub Location Problem (GHLP) as an extension of the classical hub location problem in which the total amount of emissions is minimized while considering a service time level. We first develop a nonlinear programming formulation for the GHLP and then reformulate the problem by using second order cone programming model that is also strengthened by perspective cuts. We present an extensive computational study and conduct sensitivity analyses by changing key parameters of the problem such as the maximum service time, the number of hubs, the hub-to-hub discount factors for the travel cost and travel time. We also present a comparison between the solutions of the p-hub median problem and the GHLP to assess the environmental impact of emissions on the results.

The extensive computational analyses discuss results and provide some managerial insights. First, different than the classical hub location problem, in the GHLP, increasing the number of hubs to be opened does not necessarily reduce the objective function value (the total amount of emissions) in the GHLP. Therefore, there is no guarantee that providing service with high number of hubs decreases the amount of pollution (or emissions). However, for larger sized networks, practitioners should open more hubs to guarantee the minimization of emission amount. Second, for tighter service time levels, the service provider should generally increase vehicle speeds on both spoke and hub arcs in order to route flows within the service time level, which also leads to an increase in the emission amount. Therefore, service providers should analyze trade-offs between service levels and environmental impacts. Third, while the hub-to-hub discount factor for the travel cost has a significant impact on the optimal network, the discount factor for the travel time has a less effect on the GHLP solutions in terms of hub locations and demand node assignments. Therefore, setting the discount factor for the travel cost could be more essential than setting the discount factor for the travel time. Fourth, the GHLP does reduce the total amount of emissions compared to p-hub median problem and tends to locate hubs based on their spatial locations. Thus, vehicle speeds and payloads should also be evaluated by the service providers that consider environmental impact of their transportation activities.

Acknowledgment

The authors thank two anonymous reviewers and the editor for their valuable comments on an earlier version of this paper that resulted in improved content and exposition.

Appendix A

A.1. Comprehensive modal emission model (CMEM)

Based on the CMEM, the fuel consumption rate, F_r (in g/s) can be calculated as,

$$F_r = \xi(K\Upsilon V + P/\eta)/\kappa,$$

where ξ is the fuel-to-air mass ratio, K is the engine friction factor (in kJ/rev.L), Υ is the engine speed (in rev/s), V is the engine displacement (in L), η is the efficiency parameter for diesel engines and κ is the heating value of a typical diesel fuel (kJ/g). Finally, P is the second-by-second engine power output (in kW) and can be calculated as follows:

$$P = P_{tract}/n_{tf} + P_{acc},$$

where n_{tf} is the vehicle drive train efficiency and P_{acc} is the engine power demand associated with running losses of the engine and the operation of vehicle accessories such as air conditioning usage (assumed to be zero). P_{tract} is the total tractive power requirement (in kW) and can be calculated as follows:

$$P_{tract} = (Ma + Mg\sin\theta + 0.5C_d\rho S v^2 + MgC_r\cos\theta)v/1000,$$

where M is the total weight of the vehicle (in kg) including the empty vehicle weight ω and payload, a is the instantaneous acceleration (in m/s^2), g is the gravitational constant (in m/s^2), θ is the road angle, C_d is the coefficient of aerodynamic drag, ρ is the air density (in kg/m^3), S is the frontal surface area (in m^2), v is the vehicle speed (in m/s) and C_r is the coefficient of rolling resistance.

We introduce the following parameters in order to simplify the above formulation: $\lambda = \xi/\kappa\psi$ where ψ is the conversion factor of fuel from g/s to L/s, $\gamma = 1/1000n_{tf}\eta$, $\delta = a + gsin\theta + gC_rcos\theta$ is a vehicle-arc specific constant and $\beta = 0.5C_d\rho S$ is a vehicle-specific constant. By using the new parameters, the total fuel consumption $F(v, M)$ (in L) of a vehicle traversing an arc of d units (in m) as a function of speed v and total weight M, can be given as follows:

$$F_r d/v = F(v, M) = d(\lambda K \Upsilon V/v + \lambda \gamma M \delta + \lambda \gamma \beta v^2).$$

A.2. Parameter values for comprehensive modal emission model (CMEM)

Notation	Description	Typical Values
ω	Curb weight (kg)	6350
k	Engine friction factor (kJ/rev/L)	0.2
Υ	Engine speed (rev/s)	33
V	Engine displacement (L)	5
a	Acceleration (m/s^2)	0
g	Gravitational constant (m/s^2)	9.81
θ	Road Angle	0
C_r	Coefficient of rolling resistance	0.01
C_d	Coefficient of aerodynamic drag	0.7
ρ	Air density (kg/m^3)	1.2041
S	Frontal Surface Area (m^2)	3.912
n_{tf}	Vehicle drive train efficiency	0.4
η	Efficiency parameter for diesel engines	0.9
ξ	Fuel to air mass ratio	1
κ	Heating value of a typical diesel fuel (kJ/g)	44
ψ	Conversion factor of fuel (g/s) to (L/s)	737
P_{acc}	Engine power demand	0

Appendix B

B.1. α_c analysis on the CAB dataset

α_c		0.75			0.5			0.25		
		Av. Speed			Av. Speed			Av. Speed		
T (h)	p	Spoke (km/h)	Hub (km/h)	Location	Spoke (km/h)	Hub (km/h)	Location	Spoke (km/h)	Hub (km/h)	Location
60	1	59.26	–	11	59.26	–	11	59.26	–	11
60	2	58.42	85.58	5,8	60.45	90.00	8,20	60.46	90.00	8,20
60	3	59.57	66.80	8,21,25	60.55	78.03	12,18,21	60.21	78.36	12,18,21
60	4	58.55	60.82	1,4,8,18	60.17	67.63	4,12,16,18	59.78	68.90	4,12,16,17
60	5	57.96	58.04	1,2,4,8,13	60.13	64.18	1,4,7,12,18	59.05	64.55	4,7,12,17,24
60	6	57.92	56.54	1,4,6,8,13,18	60.61	61.71	1,4,6,7,12,18	59.21	62.58	4,6,7,12,17,24
60	7	58.20	57.45	1,2,4,6,8,13,21	57.61	56.71	1,4,6,7,8,18,21	59.44	60.52	4,6,7,12,17,21,24
60	8	58.24	56.16	1,4,5,6,8,13,18,21	57.75	56.33	1,4,5,6,8,13,18,21	60.46	60.18	4,6,7,8,12,17,21,24
54	1	62.11	–	11	62.11	–	11	62.11	–	11
54	2	61.50	90.00	5,8	61.50	90.00	5,8	61.07	90.00	5,8
54	3	59.60	70.70	8,13,20	59.80	75.44	8,18,21	59.47	76.64	8,18,21
54	4	60.77	63.98	1,4,8,18	60.29	64.76	1,4,8,18	63.09	72.57	14,18,21,22
54	5	60.04	60.06	1,2,4,8,13	58.87	60.29	4,8,13,18,24	62.93	67.53	4,7,14,18,22
54	6	60.19	58.53	1,4,6,8,13,18	59.19	58.99	4,6,8,13,18,24	59.61	62.99	4,7,8,12,17,24
54	7	60.56	57.60	1,2,4,6,8,13,21	59.78	58.04	1,4,6,8,13,18,21	60.11	61.14	4,6,7,8,12,17,24
54	8	60.63	56.90	1,2,4,5,6,8,13,21	59.80	57.18	1,4,5,6,8,13,18,21	60.29	59.55	4,6,7,8,12,17,21,24
48	1		Infeasible			Infeasible			Infeasible	
48	2		Infeasible			Infeasible			Infeasible	
48	3	62.49	77.35	8,13,20	62.20	78.39	8,13,20	63.17	78.40	2,8,13
48	4	62.69	67.61	4,8,13,18	61.94	68.44	4,8,16,18	61.99	68.43	4,8,16,17
48	5	63.33	63.38	1,2,4,8,13	62.10	63.30	4,8,13,18,24	62.47	70.67	4,8,12,16,18
48	6	63.79	61.06	1,4,6,8,13,18	62.09	61.68	4,6,8,13,18,24	63.12	65.80	4,7,8,12,18,24
48	7	64.09	59.27	1,4,6,8,13,18,21	63.07	59.31	1,4,6,7,8,18,21	63.59	64.21	4,6,7,8,12,17,24
48	8	64.25	58.08	1,4,5,6,8,13,18,21	63.45	58.49	1,4,5,6,8,13,18,21	63.62	62.48	4,6,7,8,12,17,21,24
Average		60.64	64.29		60.58	66.45		61.11	69.27	

B.2. α_c analysis on the TR dataset

α_c		0.75			0.5			0.25		
		Av. Speed			Av. Speed			Av. Speed		
T (h)	p	Spoke (km/h)	Hub (km/h)	Location	Spoke (km/h)	Hub (km/h)	Location	Spoke (km/h)	Hub (km/h)	Location
24	1	59.85	–	38	59.85	–	38	59.85	–	38
24	2	58.84	90.00	6,44	58.68	90.00	6,44	59.53	90.00	26,44
24	3	58.32	66.79	1,6,23	58.27	78.39	6,34,44	57.71	78.40	6,23,34
24	4	58.04	65.29	1,6,23,26	58.11	70.58	3,5,27,34	58.08	71.25	3,21,34,38
24	5	57.74	63.35	1,3,6,23,34	57.07	63.98	1,3,6,23,34	56.27	66.87	6,20,25,27,34
24	6	56.97	59.34	1,3,5,6,23,34	56.80	61.11	1,3,6,21,34,61	56.42	63.82	1,6,20,21,34,68
24	7	56.93	58.05	1,3,5,6,23,34,68	56.44	58.59	1,3,5,6,21,25,34	56.54	61.76	1,3,6,21,34,35,61
24	8	56.65	57.28	1,3,5,6,23,25,34,68	56.77	58.52	1,3,5,6,21,25,34,35	56.20	59.09	1,3,6,21,25,34,35,55
22	1		Infeasible			Infeasible			Infeasible	
22	2	61.36	90.00	6,44	61.35	90.00	6,44	60.83	90.00	6,23
22	3	60.59	66.79	1,6,23	60.80	78.39	6,34,44	61.16	78.40	6,16,23
22	4	60.60	66.56	1,6,23,26	59.50	72.21	3,6,34,44	59.09	72.59	6,20,23,34
22	5	58.92	65.70	1,3,6,23,34	58.74	65.82	1,3,6,23,34	57.46	72.67	6,20,25,27,34
22	6	58.32	61.61	1,3,5,6,23,34	57.97	64.06	1,3,6,21,34,61	57.84	65.44	1,6,20,21,34,68
22	7	58.30	59.63	1,3,5,6,23,34,68	57.21	60.50	1,3,5,6,21,25,34	57.92	64.14	1,3,6,21,34,35,61
22	8	57.78	58.84	1,3,5,6,23,25,34,68	57.67	60.31	1,3,5,6,21,25,34,35	56.91	61.37	1,3,6,21,25,34,35,55
20	1		Infeasible			Infeasible			Infeasible	
20	2		Infeasible			Infeasible			Infeasible	
20	3		Infeasible			Infeasible			Infeasible	
20	4		Infeasible			Infeasible			Infeasible	
20	5	61.61	73.72	21,25,26,34,68	61.40	74.76	21,25,26,34,68	61.57	74.76	21,25,26,34,68
20	6	61.51	70.93	6,21,25,26,34,68	61.38	71.76	20,21,26,34,61,68	61.51	71.52	16,20,21,34,61,68
20	7	60.60	68.06	1,3,6,16,21,34,61	59.89	67.65	1,3,6,16,21,34,61	59.52	68.42	1,6,16,20,21,34,68
20	8	60.02	63.37	1,3,5,6,16,21,25,34	58.99	62.95	1,3,5,6,16,21,25,34	58.24	64.16	1,6,16,20,21,25,34,55
Average		59.10	66.96		58.78	69.42		58.56	70.81	

Appendix C

C.1. α_t analysis on the CAB dataset

α_t		0.8				0.6				0.4			
			Av. Speed				Av. Speed				Av. Speed		
T (h)	p	Emission (L)	Spoke (km/h)	Hub (km/h)	Location	Emission (L)	Spoke (km/h)	Hub (km/h)	Location	Emission (L)	Spoke (km/h)	Hub (km/h)	Location
60	1	30.66	59.26	–	11	30.66	59.26	–	11	30.66	59.25		11
60	2	22.17	58.42	85.58	5,8	22.07	59.06	88.87	5,12	21.90	57.76	71.77	5,12
60	3	20.12	59.57	66.80	8,21,25	19.98	59.57	69.97	12,21,25	19.75	57.81	60.78	12,21,25
60	4	19.18	58.55	60.82	1,4,8,18	19.11	56.98	57.63	1,2,4,8	19.07	55.78	55.75	1,4,8,18
60	5	19.17	57.96	58.04	1,2,4,8,13	19.11	56.49	56.26	1,2,4,8,13	19.09	55.32	55.26	1,2,4,8,13
60	6	19.51	57.92	56.54	1,4,6,8,13,18	19.45	56.40	55.82	1,4,6,8,13,18	19.44	55.33	55.24	1,4,6,8,13,18
60	7	20.25	58.20	57.45	1,2,4,6,8,13,21	20.17	56.47	55.64	1,4,6,8,13,18,21	20.17	55.33	55.22	1,2,4,6,8,13,21
60	8	21.20	58.24	56.16	1,4,5,6,8,13,18,21	21.14	56.72	55.57	1,2,4,5,6,8,13,21	21.22	55.34	55.22	1,2,4,5,8,9,13,21
54	1	30.88	62.11	–	11	30.88	62.11	–	11	30.88	62.11		11
54	2	22.33	61.50	90.00	5,8	22.21	59.41	85.83	5,8	22.03	59.26	82.25	5,12
54	3	20.38	59.60	70.70	8,13,20	20.14	59.92	66.77	8,21,25	19.89	59.31	65.16	12,21,25
54	4	19.33	60.77	63.98	1,4,8,18	19.19	58.89	59.97	1,4,8,18	19.11	57.01	56.89	1,4,8,18
54	5	19.29	60.04	60.06	1,2,4,8,13	19.17	58.12	57.57	1,2,4,8,13	19.11	56.27	55.79	1,2,4,8,13
54	6	19.62	60.19	58.53	1,4,6,8,13,18	19.52	58.36	56.87	1,4,6,8,18,21	19.46	56.23	55.56	1,4,6,8,13,18
54	7	20.37	60.56	57.60	1,2,4,6,8,13,21	20.22	58.19	56.24	1,4,6,8,13,18,21	20.19	56.39	55.48	1,2,4,6,8,13,21
54	8	21.31	60.63	56.90	1,2,4,5,6,8,13,21	21.19	58.58	56.03	1,2,4,5,6,8,13,21	21.14	56.35	55.39	1,4,5,6,8,13,18,21
48	1			Infeasible				Infeasible				Infeasible	
48	2			Infeasible		22.43	63.12	90.00	5,8	22.27	60.71	84.03	5,8
48	3	20.59	62.49	77.35	8,13,20	20.43	60.75	70.42	8,13,20	20.19	60.66	65.37	8,21,25
48	4	19.59	62.69	67.61	4,8,13,18	19.35	61.63	63.19	1,4,8,18	19.19	59.11	58.63	1,4,8,18
48	5	19.51	63.33	63.38	1,2,4,8,13	19.30	60.72	59.66	1,2,4,8,13	19.16	58.15	56.90	1,2,4,8,13
48	6	19.84	63.79	61.06	1,4,6,8,13,18	19.65	60.64	58.07	1,4,6,8,13,18	19.53	58.54	56.44	1,4,6,8,18,21
48	7	20.55	64.09	59.27	1,4,6,8,13,18,21	20.34	60.94	57.24	1,4,6,8,13,18,21	20.21	58.12	55.91	1,4,6,8,13,18,21
48	8	21.52	64.25	58.08	1,4,5,6,8,13,18,21	21.40	61.38	56.75	1,2,4,5,8,9,13,21	21.19	58.30	55.74	1,4,5,6,8,13,18,21
Average		21.24	60.64	64.29		21.12	59.12	62.22		21.03	57.63	59.24	

C.2. α_t analysis on the TR dataset

α_t		0.8				0.6				0.4			
			Av. Speed				Av. Speed				Av. Speed		
T (h)	p	Emission (L)	Spoke (km/h)	Hub (km/h)	Location	Emission (L)	Spoke (km/h)	Hub (km/h)	Location	Emission (L)	Spoke (km/h)	Hub (km/h)	Location
24	1	79.31	59.85	–	38	79.31	59.85	–	38	79.31	59.85		38
24	2	64.87	58.84	90.00	6,44	64.78	57.56	90.00	6,44	64.73	56.77	81.78	6,44
24	3	61.26	58.32	66.79	1,6,23	61.18	56.83	66.79	1,6,23	61.14	56.25	61.44	1,6,23
24	4	57.95	58.04	65.29	1,6,23,26	57.87	56.81	62.17	1,6,23,26	57.81	56.01	57.95	1,6,23,26
24	5	54.59	57.74	63.35	1,3,6,23,34	54.47	56.54	59.10	1,3,6,23,34	54.43	55.66	56.14	1,3,6,23,34
24	6	52.82	56.97	59.34	1,3,5,6,23,34	52.75	56.10	56.98	1,3,5,6,23,34	52.72	55.39	55.46	1,3,5,6,23,34
24	7	52.26	56.93	58.05	1,3,5,6,23,34,68	52.19	56.10	56.46	1,3,5,6,23,34,68	52.16	55.39	55.38	1,3,5,6,23,34,68
24	8	51.98	56.65	57.28	1,3,5,6,23,25,34,68	51.91	56.19	56.23	1,3,5,6,16,23,34,68	51.88	55.31	55.28	1,3,5,6,16,23,34,68
22	1			Infeasible				Infeasible				Infeasible	
22	2	65.18	61.36	90.00	6,44	64.92	59.46	90.00	6,44	64.81	57.93	90.00	6,44
22	3	61.44	60.59	66.79	1,6,23	61.28	58.67	66.79	1,6,23	61.19	57.19	65.52	1,6,23
22	4	58.12	60.60	66.56	1,6,23,26	57.97	57.94	65.01	1,6,23,26	57.86	56.85	60.41	1,6,23,26
22	5	54.68	58.92	65.70	1,3,6,23,34	54.54	57.50	61.48	1,3,6,23,34	54.46	56.32	57.48	1,3,6,23,34
22	6	52.91	58.32	61.61	1,3,5,6,23,34	52.80	56.91	58.43	1,3,5,6,23,34	52.74	55.88	56.16	1,3,5,6,23,34
22	7	52.35	58.30	59.63	1,3,5,6,23,34,68	52.24	56.88	57.43	1,3,5,6,23,34,68	52.17	55.88	55.88	1,3,5,6,23,34,68
22	8	52.06	57.78	58.84	1,3,5,6,23,25,34,68	51.96	56.37	56.52	1,3,5,6,23,25,34,68	51.89	55.81	55.64	1,3,5,6,16,23,34,68
20	1			Infeasible				Infeasible				Infeasible	
20	2			Infeasible		65.57	61.78	90.00	6,23	64.97	60.14	90.00	6,44
20	3			Infeasible		61.48	61.10	66.79	1,6,23	61.31	59.03	66.79	1,6,23
20	4			Infeasible		58.11	60.44	66.26	1,6,23,26	57.94	58.07	63.53	1,6,23,26
20	5	60.06	61.61	73.72	21,25,26,34,68	54.68	58.95	64.23	1,3,6,23,34	54.52	57.42	59.58	1,3,6,23,34
20	6	57.33	61.51	70.93	6,21,25,26,34,68	52.89	58.30	60.73	1,3,5,6,23,34	52.77	56.79	57.37	1,3,5,6,23,34
20	7	53.45	60.60	68.06	1,3,6,16,21,34,61	52.33	58.21	58.98	1,3,5,6,23,34,68	52.21	56.76	56.72	1,3,5,6,23,34,68
20	8	52.62	60.02	63.37	1,3,5,6,16,21,25,34	52.02	57.46	57.74	1,3,5,6,23,25,34,68	51.93	56.81	56.36	1,3,5,6,16,23,34,68
Average		57.65	59.10	66.96		56.95	57.51	63.62		56.88	56.54	60.81	

Appendix D

D.1. GHLP and two-stage p-HMP comparison on the CAB dataset

		Two-stage *p*-HMP		GHLP		
T (h)	p	Emission (L)	Location	Emission (L)	Location	Improvement (%)
60	1	30.66	11	30.66	11	0.00
60	2	22.61	8,20	22.17	5,8	1.99
60	3	20.42	2,4,8	20.12	8,21,25	1.52
60	4	19.88	1,4,12,18	19.18	1,4,8,18	3.62
60	5	19.80	1,4,7,12,18	19.17	1,2,4,8,13	3.28
60	6	20.73	1,4,6,7,12,17	19.51	1,4,6,8,13,18	6.26
60	7	22.16	1,4,6,7,8,12,17	20.25	1,2,4,6,8,13,21	9.39
60	8	24.08	1,4,6,7,8,12,17,25	21.20	1,4,5,6,8,13,18,21	13.56
54	1	30.88	11	30.88	11	0.00
54	2	22.33	5,8	22.33	5,8	0.00
54	3	20.52	5,8,18	20.38	8,13,20	0.66
54	4	19.32	1,4,8,18	19.33	1,4,8,18	0.00
54	5	20.50	1,4,8,12,18	19.29	1,2,4,8,13	6.27
54	6	20.97	1,4,7,8,12,18	19.62	1,4,6,8,13,18	6.84
54	7	22.34	1,4,6,7,8,12,17	20.37	1,2,4,6,8,13,21	9.69
54	8	24.28	1,4,6,7,8,12,17,25	21.31	1,2,4,5,6,8,13,21	13.93
48	1		Infeasible		Infeasible	–
48	2		Infeasible		Infeasible	–
48	3	20.59	8,13,20	20.59	8,13,20	0.00
48	4	19.91	1,4,8,18	19.59	4,8,13,18	1.63
48	5	22.01	1,4,12,18,23	19.51	1,2,4,8,13	12.83
48	6	21.29	1,4,7,8,12,18	19.84	1,4,6,8,13,18	7.31
48	7	22.70	1,4,6,7,8,12,17	20.55	1,4,6,8,13,18,21	10.45
48	8	24.68	1,4,6,7,8,12,17,25	21.52	1,4,5,6,8,13,18,21	14.70
Average		22.39		21.24		5.63

D.2. GHLP and two stage p-HMP comparison on the TR dataset

		Two-stage *p*-HMP		GHLP		
T (h)	p	Emission (L)	Location	Emission (L)	Location	Improvement (%)
24	1	79.31	38	79.31	38	0.00
24	2	65.88	6,38	64.87	6,44	1.56
24	3	62.29	3,34,38	61.26	1,6,23	1.68
24	4	58.90	3,6,34,38	57.95	1,6,23,26	1.63
24	5	54.70	1,3,6,23,34	54.59	1,3,6,23,34	0.21
24	6	52.87	1,3,5,6,23,34	52.82	1,3,5,6,23,34	0.09
24	7	52.51	1,3,5,6,16,23,34	52.26	1,3,5,6,23,34,68	0.48
24	8	52.33	1,3,5,6,16,23,34,35	51.98	1,3,5,6,23,25,34,68	0.66
22	1		Infeasible		Infeasible	–
22	2	65.18	6,44	65.18	6,44	0.00
22	3	61.47	1,6,23	61.44	1,6,23	0.05
22	4	58.17	1,6,23,26	58.12	1,6,23,26	0.08
22	5	54.78	1,3,6,23,34	54.68	1,3,6,23,34	0.18
22	6	52.97	1,3,5,6,23,34	52.91	1,3,5,6,23,34	0.10
22	7	52.62	1,3,5,6,16,23,34	52.35	1,3,5,6,23,34,68	0.52
22	8	52.45	1,3,5,6,16,23,34,35	52.06	1,3,5,6,23,25,34,68	0.75
20	1		Infeasible		Infeasible	–
20	2		Infeasible		Infeasible	–
20	3		Infeasible		Infeasible	–
20	4		Infeasible		Infeasible	–
20	5	60.10	21,25,26,34,68	60.06	21,25,26,34,68	0.07
20	6	57.40	6,21,25,26,34,68	57.33	6,21,25,26,34,68	0.11
20	7	53.51	1,3,6,16,21,34,61	53.45	1,3,6,16,21,34,61	0.12
20	8	52.75	1,3,5,6,16,21,25,34	52.62	1,3,5,6,16,21,25,34	0.25
Average		57.91		57.65		0.45

References

Alumur, S., Kara, B.Y., 2008. Network hub location problems: The state of the art. Eur. J. Oper. Res. 190, 1–21.

Alumur, S.A., Kara, B.Y., Karasan, O.E., 2009. The design of single allocation incomplete hub networks. Transport. Res. Part B: Methodol. 43, 936–951.

Alumur, S.A., Kara, B.Y., Karasan, O.E., 2012a. Multimodal hub location and hub network design. Omega 40, 927–939.

Alumur, S.A., Yaman, H., Kara, B.Y., 2012b. Hierarchical multimodal hub location problem with time-definite deliveries. Transport. Res. Part E: Logist. Transport. Rev. 48, 1107–1120.

Barbosa-Póvoa, A.P., da Silva, C., Carvalho, A., 2018. Opportunities and challenges in sustainable supply chain: An operations research perspective. Eur. J. Oper. Res. 268, 399–431.

Barth, M., Boriboonsomsin, K., 2008. Real-world carbon dioxide impacts of traffic congestion. Transport. Res. Rec.: J. Transport. Res. Board 2058, 163–171.

Barth, M., Younglove, T., Scora, G., 2005. Development of a heavy-duty diesel modal emissions and fuel consumption model. Technical Report California Partners for Advanced Transit and Highways (PATH), Institute of Transportation Studies, University of California at Berkeley.

Beasley, J.E., 2012. Or-library: Hub location. http://people.brunel.ac.uk/mastjjb/jeb/orlib/phubinfo.html. Accessed: 2018-08-17.

Bektaş, T., Laporte, G., 2011. The pollution-routing problem. Transport. Res. Part B: Methodol. 45, 1232–1250.

Campbell, J.F., 1994. Integer programming formulations of discrete hub location problems. Eur. J. Oper. Res. 72, 387–405.

Campbell, J.F., 2009. Hub location for time definite transportation. Comput. Oper. Res. 36, 3107–3116.

Daryanto, Y., Wee, H.M., Astanti, R.D., 2019. Three-echelon supply chain model considering carbon emission and item deterioration. Transport. Res. Part E: Logist. Transport. Rev. 122, 368–383.

Demir, E., Bektaş, T., Laporte, G., 2012. An adaptive large neighborhood search heuristic for the Pollution-Routing Problem. Eur. J. Oper. Res. 223, 346–359.

Demir, E., Bektaş, T., Laporte, G., 2014. A review of recent research on green road freight transportation. Eur. J. Oper. Res. 237, 775–793.

Dukkanci, O., Bektaş, T., Kara, B.Y., 2019. Green network design problems. In: Faulin, J., Grasman, S.E., Juan, A.A., Hirsch, P. (Eds.), Sustainable Transportation and Smart Logistics. Elsevier, pp. 169–206.

Dukkanci, O., Kara, B.Y., 2017. Routing and scheduling decisions in the hierarchical hub location problem. Comput. Oper. Res. 85, 45–57.

Ernst, A.T., Jiang, H., Krishanmoorthy, M., Baatar, D., 2018. Reformulations and computational results for the uncapacitated single allocation hub covering problem. In: Sarker, R., Abbass, H.A., Dunstall, S., Kilby, P., Davis, R., Young, L. (Eds.), Data and Decision Sciences in Action. Lecture Notes in Management and Industrial Engineering. Springer, pp. 133–148.

Farahani, R.Z., Hekmatfar, M., Arabani, A.B., Nikbakhsh, E., 2013. Hub location problems: A review of models, classification, solution techniques, and applications. Comput. Ind. Eng. 64, 1096–1109.

Govindan, K., Jafarian, A., Khodaverdi, R., Devika, K., 2014. Two-echelon multiple-vehicle location-routing problem with time windows for optimization of sustainable supply chain network of perishable food. Int. J. Prod. Econ. 152, 9–28.

Günlük, O., Linderoth, J., 2012. Perspective reformulation and applications. In: Lee, J., Leyffer, S. (Eds.), Mixed Integer Nonlinear Programming. Springer, pp. 61–89.

Hamacher, H.W., Meyer, T., 2006. Hub cover and hub center problems. Department of Mathematics, University of Kaiserslautern Gottlieb-Daimler-Strasse, 67663 Kaiserslautern, Germany. Technical Report. https://kluedo.ub.uni-kl.de/frontdoor/deliver/index/docId/1748/file/Nr.98.pdf.

Ishfaq, R., Sox, C.R., 2011. Hub location-allocation in intermodal logistic networks. Eur. J. Oper. Res. 210, 213–230.

Kara, I., Kara, B.Y., Yetis, M.K., 2007. Energy minimizing vehicle routing problem. In: Dress, A., Yinfeng, X., Binhai, Z. (Eds.), Combinatorial Optimization and Applications. Lecture Notes in Computer Science, vol. 4616. Springer Berlin Heidelberg, pp. 62–71.

Kaya, O., Urek, B., 2016. A mixed integer nonlinear programming model and heuristic solutions for location, inventory and pricing decisions in a closed loop supply chain. Comput. Oper. Res. 65, 93–103.

Khoei, A.A., Süral, H., Tural, M.K., 2017. Time-dependent green weber problem. Comput. Oper. Res. 88, 316–323.

Koç, Ç., Bektaş, T., Jabali, O., Laporte, G., 2016. The impact of depot location, fleet composition and routing on emissions in city logistics. Transport. Res. Part B: Methodol. 84, 81–102.

Lin, C.-C., Chen, S.-H., 2004. The hierarchical network design problem for time-definite express common carriers. Transport. Res. Part B: Methodol. 38, 271–283.

Lobo, M.S., Vandenberghe, L., Boyd, S., Lebret, H., 1998. Applications of second-order cone programming. Linear Algebra Appl. 284, 193–228.

Mohammadi, M., Torabi, S., Tavakkoli-Moghaddam, R., 2014. Sustainable hub location under mixed uncertainty. Transport. Res. Part E: Logist. Transport. Rev. 62, 89–115.

Niknamfar, A.H., Niaki, S.T.A., 2016. Fair profit contract for a carrier collaboration framework in a green hub network under soft time-windows: Dual lexicographic max–min approach. Transport. Res. Part E: Logist. Transport. Rev. 91, 129–151.

O'Kelly, M.E., 1986a. Activity levels at hub facilities in interacting networks. Geograph. Anal. 18, 343–356.

O'Kelly, M.E., 1986b. The location of interacting hub facilities. Transport. Sci. 20, 92–106.

O'Kelly, M.E., 1987. A quadratic integer program for the location of interacting hub facilities. Eur. J. Oper. Res. 32, 393–404.

Rahimi, M., Baboli, A., Rekik, Y., 2017. Multi-objective inventory routing problem: A stochastic model to consider profit, service level and green criteria. Transport. Res. Part E: Logist. Transport. Rev. 101, 59–83.

Rohmer, S., Gerdessen, J., Claassen, G., 2019. Sustainable supply chain design in the food system with dietary considerations: A multi-objective analysis. Eur. J. Oper. Res. 273, 1149–1164.

Saberi, S., 2018. Sustainable, multiperiod supply chain network model with freight carrier through reduction in pollution stock. Transport. Res. Part E: Logist. Transport. Rev. 118, 421–444.

Sbihi, A., Eglese, R.W., 2010. Combinatorial optimization and green logistics. Ann. Oper. Res. 175, 159–175.

Scora, G., Barth, M., 2006. Comprehensive modal emissions model, version 3.01 User's guide. Technical Report Centre for Environmental Research and Technology. University of California, Riverside, United States of America.

Tan, P.Z., Kara, B.Y., 2007. A hub covering model for cargo delivery systems. Networks: Int. J. 49, 28–39.

Tricoire, F., Parragh, S.N., 2017. Investing in logistics facilities today to reduce routing emissions tomorrow. Transport. Res. Part B: Methodol. 103, 56–67.

Yaman, H., 2009. The hierarchical hub median problem with single assignment. Transport. Res. Part B: Methodol. 43, 643–658.

Zhalechian, M., Tavakkoli-Moghaddam, R., Zahiri, B., Mohammadi, M., 2016. Sustainable design of a closed-loop location-routing-inventory supply chain network under mixed uncertainty. Transport. Res. Part E: Logist. Transport. Rev. 89, 182–214.

Zhang, T., Choi, T.-M., Zhu, X., 2018. Optimal green product's pricing and level of sustainability in supply chains: effects of information and coordination. Ann. Oper. Res. 1–26. https://doi.org/10.1007/s10479-018-3084-8.